

## INDICE

Editorial .....	1
Preparation, characterization and study of morphology of activated carbon fibers .....	2
Activated carbons as catalyst in the synthesis of fine chemicals .....	7
Adsorption of phenol from aqueous solution by activated carbons derived from cherry stones .....	11
Activated carbons developed in different activation conditions to improve nitrate adsorption performance .....	16
Preparation of activated carbon-metal (hydr)oxide photocatalysts under different heating conditions. Chemical aspects .....	22
Reseña Tesis. Electrochemically modified carbon materials for applications in electrocatalysis and biosensors .....	27
Reseña Tesis. Doped carbon material electrodes for energy applications .....	30

Editor Jefe:

**F. José Maldonado Hódar**  
 Universidad de Granada

Editores:

**Miguel Montes**  
 INCAR. Oviedo

**Patricia Álvarez**  
 INCAR. Oviedo

**Olga Guerrero**  
 Universidad de Málaga

**Jorge Bedia**  
 Universidad Autónoma Madrid

**M. Ángeles Lillo-Ródenas**  
 Universidad de Alicante

**Manuel Sánchez-Polo**  
 Universidad de Granada

**Isabel Suelves**  
 ICB-CSIC, Zaragoza

Editor invitado:

**Vicente Gómez Serrano**  
 Universidad de Extremadura

# BOLETIN del Grupo Español del Carbón

ISSN 2172 - 6094  
 nº 42/Diciembre 2016

## Editorial

En la Universidad de Extremadura (UEx), la investigación en el amplio campo de los materiales carbonosos tuvo su comienzo en los primeros años de la década de los ochenta cuando los Profesores Ángel Linares Solano y Concepción Martínez de Lecea, en el breve periodo de tiempo que permanecieron en esta universidad, instalaron dos aparatos de adsorción física de gases, uno gravimétrico y otro volumétrico, en uno de los laboratorios del Departamento de Química Inorgánica para sus investigaciones sobre carbones minerales.

Dichos aparatos fueron después utilizados en beneficio de los que nos incorporamos después al permitir que se pudieran realizar estudios de caracterización de sólidos porosos, sin apenas dilación.

Desde entonces, no solo en el citado Departamento de Química Inorgánica, sino también en los Departamentos de Ingeniería Mecánica, Energética y de los Materiales, Ingeniería Química y Química Física, y de Física Aplicada han ido emergiendo grupos de investigación, en la mayoría de los casos tras una relación previa con el grupo del Departamento de Química Inorgánica (Grupo de Adsorbentes Carbonosos. Adsorción, Grupo ACA), los cuales han centrado cada vez más la investigación en los materiales carbonosos.

En particular, la intensa labor investigadora realizada en este campo ha tratado sobre la preparación de adsorbentes carbonosos a partir de un elevado número de materiales de partida de origen vegetal e industrial y sobre la caracterización físico química y textural y las aplicaciones de los productos obtenidos, sobre todo en la retención de solutos de naturaleza orgánica e inorgánica en disolución acuosa. Un buen ejemplo de ello son los artículos recogidos en el presente número de la revista del Grupo Español del Carbón, los cuales tratan sobre temas de investigación tradicionales y más avanzados y novedosos con materiales carbonosos.

Otras líneas de investigación más actuales que se desarrollan con dichos materiales se basan en la utilización o técnicas de hidrocarbonización en su preparación, la obtención de productos magnéticos, el empleo como catalizadores y en procesos de electroadSORCIÓN, como supercondensadores, etc.

Nuestro agradecimiento al Grupo Editor de la Revista del Grupo Español de Carbón por la invitación a dar a conocer en parte, al menos, la investigación que se realiza actualmente en la UEx.

*Prof. Vicente Gómez Serrano*

***Feliz Navidad a todos***

***Que la paz y los buenos deseos nos duren todo el año***



# Preparation, characterization and study of morphology of activated carbon fibers

## Preparación, caracterización y estudio morfológico de fibras de carbón activado

**A. Macías-García<sup>a</sup>, M. Alexandre Franco<sup>b</sup>, M. Alfaro Domínguez<sup>a\*</sup>, J. Martínez Naharro<sup>a</sup>, V. Encinas-Sánchez<sup>a</sup>**

<sup>a</sup> Departamento de Ingeniería Mecánica, Energética y de los Materiales, Universidad de Extremadura, Avda. de Elvas s/n, E-06071-Badajoz, Spain

<sup>b</sup> Departamento de Química Orgánica e Inorgánica, Universidad de Extremadura, Avda. de Elvas s/n, E-06071-Badajoz, Spain

### Abstract

Using kenaf as starting material, a study about the preparation and characterization of activated carbon fibers (ACFs) from long fibers was carried out. The carbonization products of kenaf fibers and ACFs were texturally characterized by N<sub>2</sub> adsorption at -196 °C, mercury porosimetry, and scanning electron microscopy.

The activation of the raw material of Kenaf by its carbonization at 400 °C for 0.5 h in a N<sub>2</sub> atmosphere increase the porosity of the samples, particularly the activation at 700 °C with carbon dioxide. It should be noted the porous development shown by the scanning electron micrographs of samples FBC4A72 and FBC4A74. It is observed that the variation of treatment time from 2 to 4 hours leads to an important development of the porous structure in samples FBC4A74, which is probably a consequence of an interconnection between pores. These results open a wide field of applications of these fibers.

### Resumen

Utilizando fibras de kenaf larga, se ha llevado a cabo la preparación, caracterización y estudio morfológico de las fibras de carbón activado (ACFs). La caracterización era realizada mediante las isotermas de adsorción de N<sub>2</sub> a -196 C, porosimetría de Hg y microscopía electrónica de barrido. La activación a 700 °C con CO<sub>2</sub> durante 2h (FBC4A72) y 4 h (FBC4A74) de la muestra carbonizada a 400 °C durante 0.5 h en N<sub>2</sub> (FBC4), mostraban un incremento en el tamaño del poro, como se observa en las microscopías electrónica de barrido. Esto es probablemente debido a la interconexión de los poros como consecuencia del incremento del tiempo de tratamiento de 2 a 4h. Estos resultados abren un amplio campo de aplicación para las fibras de kenaf.

### 1. Introduction

Activated carbon fibers (ACFs) constitute a particular type of activated carbon, the morphology of ACF being fibrous in nature. ACFs present certain specific advantages in comparison to other activated carbons. Because of their large surface area, porous character and high adsorption/desorption rate they are widely used as adsorbents in numerous applications [1].

A potential precursor of ACFs is Kenaf, possesses two types of fibers: the bark and the woody nuclei, which represent about 30 % and 70 % of the crop, respectively. So far, these fibers have been mostly used to obtain textile and paper products, which compete strongly with wood and synthetic fibers. As a result, the possibility of using natural fibers in other

applications has not been developed extensively [2,3]. The main objective of the present work was to carry out the preparation and characterization of ACFs obtained from Kenaf.

### 2. Experimental

#### 2.1. Starting material

Kenaf (2-3 cm diameter trunks) supplied by the Junta de Extremadura (Spain) was used. The received trunks were air-dried, that easily enables isolate, either manually or mechanically, the long fibers (outer part) from the short fibers (inner part) and then the longer fibers one by one. After this step, only the longer fibers (KFs, hereafter) were selected for subsequent studies.

#### 2.2. Chemical analyses of KFs

The cellulose, hemicellulose and lignin content were determined by the Tappi method [4,5].

Data of the proximate analysis of KFs (Table 1) were obtained using a thermogravimetric method [6] and elemental analysis was performed on a dry basis using a model CE440 Elemental Analyzer (Table 1).

#### 2.3. Carbonization of KFs

The carbonization of KFs was developed in a tubular furnace consisting of a Termolab with Eurotherm 904 temperature controllers and a 1 meter-tubular ceramic inserted. About 1.5 g of KFs was placed in a 10 cm stainless steel boat with perforated ends to facilitate gas flow. The boat was positioned in the centre of the constant temperature zone. The carbonization of the fibres was carried out at 300 and 400° C in N<sub>2</sub> atmosphere (flow rate of 85 mL min<sup>-1</sup>). The heating rate from room temperature to the maximum heat temperature (MHTT) was 5 °C min<sup>-1</sup>. The heating time at MHTT was 0.5 and 1 h. The notations used for the carbonized fibers (CFs) were FBCT fibers carbonized at 300-400°C for 0.5 h and FBCT1 carbonized fibers carbonized at 300-400°C for 1 h; T will be equal to 3 o 4 as a function of the temperature (3 in the case of a temperature of 300 °C and 4 in the case of 400 °C).

#### 2.4. Preparation of ACFs

Using the same calefaction system used in the carbonization treatments, the fiber carbonized at 400 °C for 0.5 h (FBCT) was used as intermediate product and was activated at 500, 600 and 700° C in a carbon dioxide atmosphere (flow rate = 85 mL min<sup>-1</sup>). The heating rate was 5 °C min<sup>-1</sup>, and the soaking time was 2 and 4 h. The notations used was FBC4ATt, where FBC4 represents fibers carbonized at 400°C for 0.5h, A, represents the activation with carbon dioxide, T is

the activation temperature (500-700°C), and t is the activation time (2 or 4 h).

## 2.5. Characterization

The characterization of CFs and ACFs was carried out by physical adsorption of N<sub>2</sub> at -196 °C. The adsorption isotherms were measured using a Quantachrome apparatus (Autosorb 1). From such isotherms, the specific surface area ( $S_{BET}$ ) was calculated by applying the BET equation [7]. The micropore volume ( $W_0$ ) was obtained using the Dubinin-Radushkevich equation [8]. Also, the micropore volume ( $V_{mi}$ ) was derived by simply reading the volume adsorbed ( $V_{ad}$ ) at  $P/P^0=0.1$  and the mesopore volume ( $V_{me}$ ) by subtraction of  $V_{mi}$  from  $V_{ad}$  at  $P/P^0=0.95$ ;  $W_0$ ,  $V_{mi}$ , and  $V_{me}$  being expressed as liquid volumes. Finally, the pore size distribution in the micropore and mesopore ranges was obtained using the Density Functional Theory (DFT) [9] and BJH methods [10]. On the other hand, information about the meso- and macroporous structures of selected ACFs was obtained by mercury porosimetry, using a Micromeritics porosimeter in the range of 0.10 – 441 MPa. The sample morphology was observed by scanning electron microscopy (SEM) using a S-3600N microscope (Hitachi, Japan).

## 3. Results and discussion

### 3.1. Chemical composition of KFs

Numerous studies performed by other authors (Stone J, Scallan A, Duchesne, and Daniel G.) show the important role that plays the contents of lignin and hemicellulose within the Kenaf in the development of its porous structure. Thus, it is observed that the reduction in lignin and hemicellulose content is directly related to the development of the porous structure [11,12]. Lignin is a natural adhesive that contains aromatic rings. These rings does not contribute to the porous development at low temperatures, nevertheless the higher temperatures favor the porous development.

The content in cellulose (69.8%), hemicellulose (12.6%) and lignin (17.6%) seem to indicate that the Kenaf fiber can be an excellent precursor in the preparation of ACFs, not finding any work related to this aspect in bibliography [13-15].

Results obtained in the proximate analysis of KFs (Table 1) indicate that this material is largely composed of volatile matter and has a low inorganic fraction. Despite the low value of fixed C, we find possible the preparation of activated carbon fibers. The special characteristics of the fibers obtained, tubular structures, would allow set functional groups and improve their absorbent properties.

**Table 1.** Proximate analyses and elemental analysis of Kenaf fibers.

**Tabla 1.** Análisis aproximado y elemental de fibras de Kenaf.

	Proximate analysis, wt.%		Elemental analysis, wt.%
Moisture	10.3	C	55.3
Volatile matter	74.0	O	39.3
Ashes <sup>a</sup>	2.7	N	0.3
Fixed carbon	13.0	H	5.1

<sup>a</sup> Average value of triplicate analyses.

The elemental analysis (Table 1) seems to indicate that the high content of volatile matter (74%) could be related to the transformation of an important part of the carbon present in the raw material (55.3%) in volatile, which would justify the value of fixed carbon obtained.

### 3.2. Textural characterization of carbonized fibers

Figure 1 shows the N<sub>2</sub> adsorption isotherms determined for the carbonized fibers. They reveal that the extent of N<sub>2</sub> adsorption is lower in FBC31 and FBC41 than FBC3 and FBC4, and also that the larger adsorption capacity correspond to FBC4.

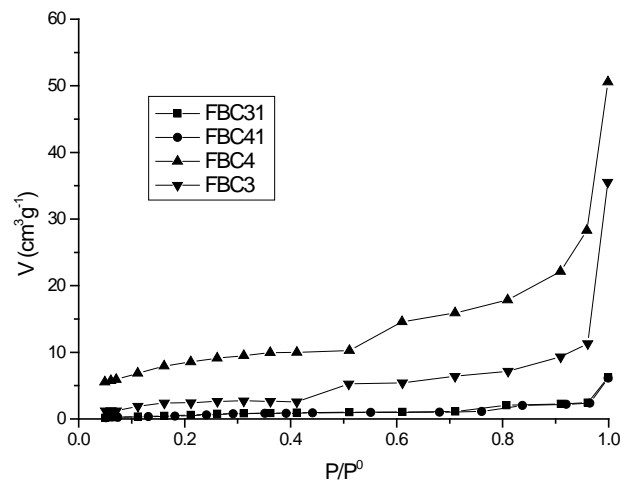


**Figure 1.** Adsorption isotherms of N<sub>2</sub> at -196°C of the carbonized fibers.

**Figura 1.** Isotermas de adsorción de N<sub>2</sub> a -196°C de fibras carbonizadas.

The shape of the isotherms resembles the type IV isotherms of the well-known BDDT classification system. Accordingly, the carbonized fibers are principally mesoporous carbons.

The textural parameters corresponding to the carbonized fibers are gathered in the Table 2.

$S_{BET}$  ranges between 3 m<sup>2</sup> g<sup>-1</sup> for FBC31 and FBC41 and 29 m<sup>2</sup> g<sup>-1</sup> for FBC4. The microporous volume, both  $V_{mi}$  and  $V_{DR}$ , is very low in all samples. The largest value of  $V_{mi}$  (0.011 cm<sup>3</sup> g<sup>-1</sup>) corresponds to

**Table 2.** Textural parameters of the carbonized fibers.

**Tabla 2.** Parámetros texturales de las fibras carbonizadas

Sample	$S_{BET}$ (m <sup>2</sup> g <sup>-1</sup> )	$W_0$ (cm <sup>3</sup> g <sup>-1</sup> )	$V_{mi}$ (cm <sup>3</sup> g <sup>-1</sup> )	$V_{me}$ (cm <sup>3</sup> g <sup>-1</sup> )	$V_{me-p}$ (cm <sup>3</sup> g <sup>-1</sup> )	$V_{ma-p}$ (cm <sup>3</sup> g <sup>-1</sup> )	APS (Å)
FBC3	8	0.005	0.003	0.015	0.010	0.021	8.57
FBC4	29	0.016	0.011	0.030	0.031	0.034	6.85
FBC31	3	0.001	0.0001	0.007	0.009	0.017	10.48
FBC41	3	0.001	0.0001	0.009	0.010	0.028	10.49

FBC4. In contrast,  $V_{me}$  is as high as  $0.030 \text{ cm}^3 \text{ g}^{-1}$  for FBC4.

From DFT plots obtained for the carbonized fibers (Fig. 2a) it is concluded that the pore size distribution is bimodal for FBC3 and FBC4. Notice that the pore size distribution in the regions of micropore and narrower mesopores is much wider in FBC4 than in FBC3. Furthermore, the larger mesopores present in these products are wider in FBC4. Thus, the more prominent peaks are located at  $19.5$  and  $37.4 \text{ \AA}$  for FBC3 and at  $17.5$  and  $46.2 \text{ \AA}$  for FBC4. From these results it becomes clear that the increase in the carbonization temperature provided that the heating time is short, gives rise to the creation and widening of pores. As far as the DFT plots for FBC3 and FBC4, they only display a single peak at close values of the pore width, which is centred between  $25$  and  $30 \text{ \AA}$ . These results suggest that when the carbonization of Kenaf fibers at  $300$  and  $400^\circ \text{C}$  is carried out for  $1 \text{ h}$  instead of  $0.5 \text{ h}$ , the widest mesopores disappear from the resultant products as a result of the increased devolatilization of the material and narrow mesopores are created, perhaps because of the widening of micropores.

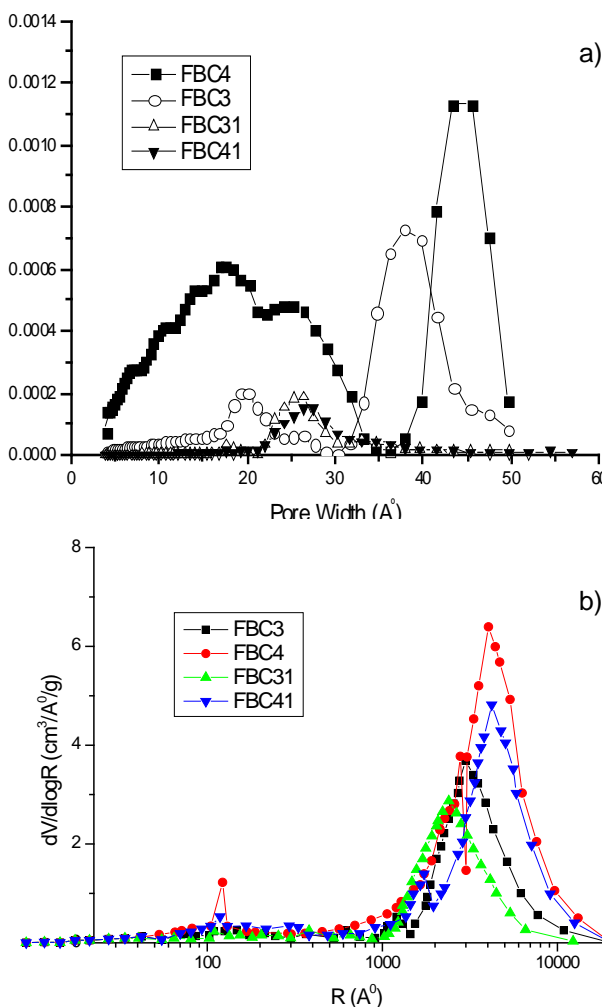


**Figure 2.** (a) DFT for the carbonized fibers, (b) Mercury porosimetry of the carbonized fibers

**Figura 2.** (a) DFT para fibras carbonizadas, (b) Porosimetría de mercurio de fibras carbonizadas

Figure 2b shows the pore size of carbonized fibers determined by mercury porosimetry. This distribution shows a peak at  $130 \text{ \AA}$  and a small mercury intrusion in the mesopore region for the samples.

### 3.3. Textural characterization of activated carbon fibers

The  $\text{N}_2$  adsorption isotherm at  $77 \text{ K}$  measured in the samples are shown in Figure 3. Isotherms are type IV according to the classification of BDDT. This figure shows the influence of two parameters: activation temperature ( $500\text{-}700^\circ \text{C}$ ) and time of treatment ( $2 \text{ y } 4 \text{ h}$ ).

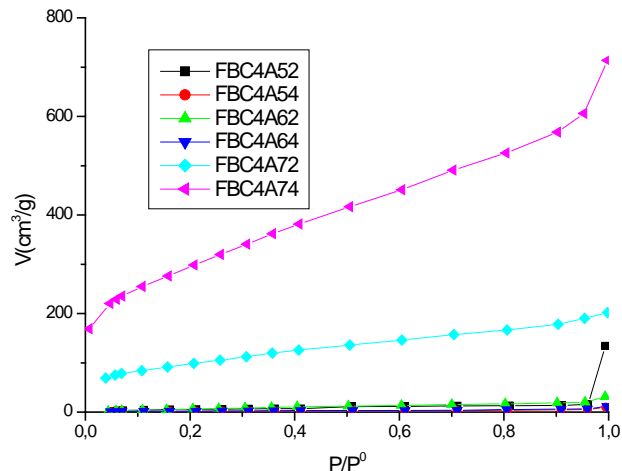


**Figure 3.** Adsorption isotherms of  $\text{N}_2$  at  $-196^\circ \text{C}$  of the activated carbon fibers.

**Figura 3.** Isoterra de adsorción de  $\text{N}_2$  at  $-196^\circ \text{C}$  de fibras de carbón activado.

On the one hand, it is observed that the isotherms obtained in the temperature range of  $500\text{-}600^\circ \text{C}$  and after  $2\text{h}$  of constant treatment are very close to the x-axis, which indicates a low development of the specific surface ( $21 \text{ m}^2 \text{ g}^{-1}$  and  $33 \text{ m}^2 \text{ g}^{-1}$  respectively) Table 3. At temperatures of  $700^\circ \text{C}$  this parameters are remarkably increased ( $341 \text{ m}^2 \text{ g}^{-1}$  in sample FBC4A72). However heat treatments for  $4 \text{ h}$  lead to a similar behavior to the previously observed with low values of specific surface in the range of  $500\text{-}600^\circ \text{C}$  and very high values after the treatment at  $700^\circ \text{C}$  (FBC4A74,  $1031 \text{ m}^2 \text{ g}^{-1}$ ). These results are better than the previously found for similar ACFs in bibliography [16, 17], although in the present study lower temperatures have been used in the activation. Thus, for example, Gaur et al. [16] prepared ACFs by physical activation at temperatures of  $800\text{-}1000^\circ \text{C}$ . The maximum value of  $S_{BET}$  obtained at these temperatures was of  $928 \text{ m}^2 \text{ g}^{-1}$ . Using similar temperatures ( $800\text{-}1000^\circ \text{C}$ ) Ko et al. [17] prepared fibers of the coal obtaining maximum  $S_{BET}$  values of  $161 \text{ m}^2 \text{ g}^{-1}$ . This behavior can be attributed to the own structure of Kenaf consisting of layers and to their contents in cellulose, lignin and hemicellulose. The values of  $S_{BET}$  obtained for the samples treated at  $700^\circ \text{C}$  during  $2$  and  $4 \text{ h}$  are quite similar to the values obtained by other authors using diverse fibers [18, 20].

If we compared the obtained textural parameters of porosity with other values obtained for other fibers rich in cellulose such as rayon [18] ( $V_{mi} = 0.68 \text{ cm}^3/\text{g}$ ,  $V_{me} = 0.32 \text{ cm}^3/\text{g}$ ), we found high values for fibers obtained from Kenaf ( $V_{mi} = 0.594 \text{ cm}^3/\text{g}$ ,  $V_{me} = 0.544 \text{ cm}^3/\text{g}$ ). The good behavior of both fibers can obey to the composition with raw materials rich in cellulose. Furthermore, it is important to highlight that the porous development of this material is obtained when it works at low temperature,  $700^\circ \text{C}$ . This fact

**Table 3.** Textural parameters of the activated carbon fibers.  
**Tabla 3.** Parámetros texturales de fibras de carbón activado.

Sample	$S_{BET}$ ( $\text{m}^2 \text{g}^{-1}$ )	$W_0$ ( $\text{cm}^3 \text{g}^{-1}$ )	$V_{mi}$ ( $\text{cm}^3 \text{g}^{-1}$ )	$V_{me}$ ( $\text{cm}^3 \text{g}^{-1}$ )	$V_{me-p}$ ( $\text{cm}^3 \text{g}^{-1}$ )	$V_{ma-p}$ ( $\text{cm}^3 \text{g}^{-1}$ )	APS ( $\text{\AA}$ )
FBC4A52	21	0.012	0.007	0.018	0.020	0.036	9.36
FBC4A54	7	0.004	0.002	0.006	0.006	0.040	8.98
FBC4A62	33	0.016	0.016	0.026	0.024	0.048	11.00
FBC4A64	8	0.005	0.003	0.080	0.092	0.060	8.78
FBC4A72	341	0.181	0.130	0.164	0.154	0.021	5.83
FBC4A74	1031	0.551	0.594	0.544	0.501	0.018	5.96

is reviewed by other authors in materials with an elevated content of lignin ( $V_{mi} = 0.53 \text{ cm}^3/\text{g}$ ) [19].

The porosity values ( $V_{mi} = 0.594 \text{ cm}^3/\text{g}$ ,  $V_{me} = 0.544 \text{ cm}^3/\text{g}$ ) obtained for Kenaf at 700° C and variable times of treatment are superior to the values found in bibliography [18-20]. The effect of the time affects in a different way and in a larger magnitude at 700° C.

On the other hand, the size distributions in micro, meso and macropores shown in Figures 4 y 5 and present two different behaviors.

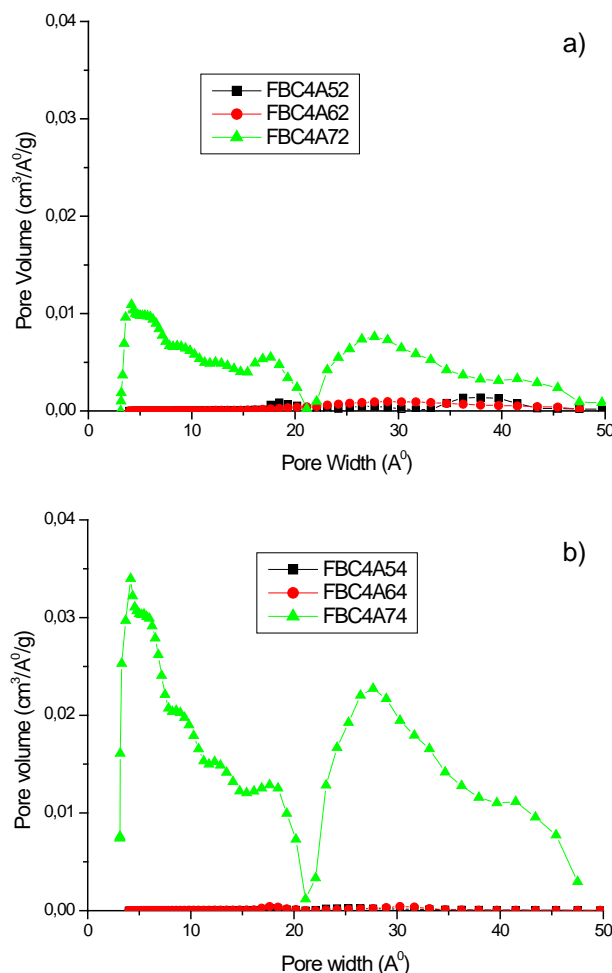


Figure 4. (a) DFT for the activated carbon fibers (2h) and (b) (4h).  
Figura 4. (a) DFT de fibras de carbón activado (2h) and (b) (4h).

The value obtained in the range temperature of 500-600° C with a time of constant treatment of 2h, is very close to the x-axis, which indicates a low development of micropores and mesopores. At temperatures of 700° C (Fig. 4a) these parameters are remarkably increased (4.17 Å and 28.4 Å) in sample FBC4A72. However, when heat treatments are maintained for

4 h, a similar behavior is observed, but with slightly lower values than in the previous case.

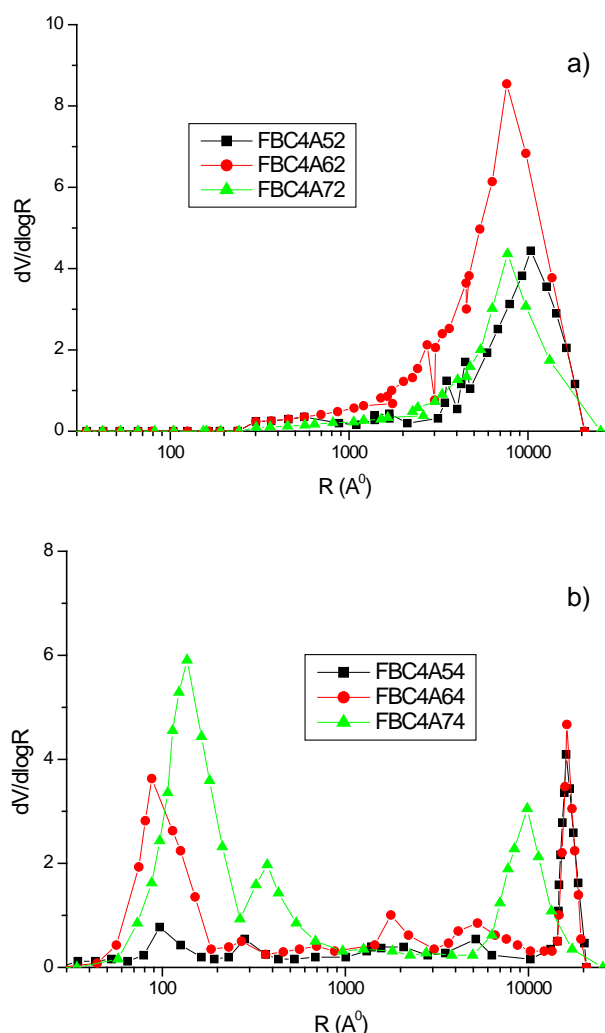


Figure 5. Mercury porosimetry of the activated carbon fibers a) 2h and b) 4h

Figura 5. Porosimetría de mercurio de fibras de carbón activado (a) 2h y (b) 4h

The results of the mercury porosimetry shown in Figs. 5a and 5b presents two noticeable behaviors depending on the studied variables (temperature and time). Thus, when the temperature of treatment is analyzed, a low development of porosity is observed but it is slightly superior for the samples treated at temperatures under 700° C, especially in the band of macropores. When we study the effect of the treatment time, it is observed that low porous development (in the strip of the mesopores) corresponds to times of 2 h, in the strip of the mesopores; however, greater porous development corresponds to times of 4 h,

pores being distributed in the zone of mesopores and macropores.

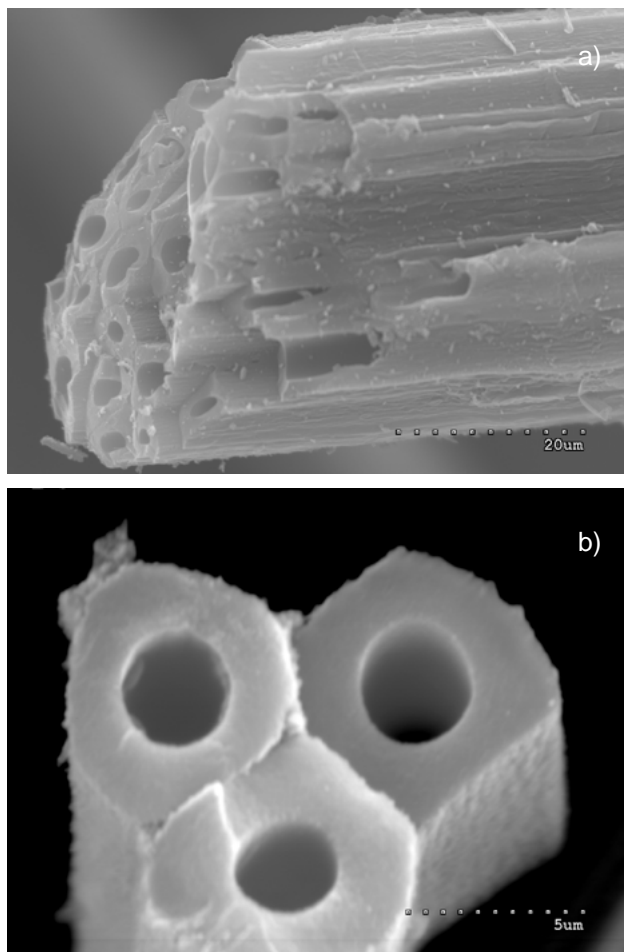


Figure 6. SEM micrograph of sample (a) FBC4A72 and (b) FBC4A74.

Figura 6. Micrografía SEM de las muestras (a) FBC4A72 and (b) FBC4A74.

Finally, with the aim of corroborating the tendencies of porous development observed in the previous sections, the morphologic evolution of pores throughout all the prepared series was studied. Special attention was focused on the samples prepared at 700°C (Fig.6a and Fig.6b). Thus, by comparing micrographs of FBC4A72 (Fig.6a) with the FBC4A74 (Fig.6b), a marked porous development was observed in the samples. A subsequent comparison of these samples with respect to the treatment time (activation at 700°C and 2h and 4h of treatment) (Fig. 6a and 6b) reflects a homogenous and uniform distribution of macropores and a greater size of pore of the sample FBC4A74. Probably, this effect obeys to the interconnection of pores and to the treatment time. These results open a wide field of applications for these types of fibers.

#### 4. Conclusions

The activation of the raw material of Kenaf by its carbonization at 400 °C during 0.5 h in N<sub>2</sub> atmosphere develops the porosity of the samples. The activation at 700 °C under carbon dioxide atmosphere, both during 2 h and during 4 h, provokes greater values of textural parameters S<sub>BET</sub>, W<sub>o</sub>, V<sub>mi</sub> and V<sub>me</sub> than the provoked to the activation at inferior temperatures (500 and 600 °C). Furthermore, results obtained at an activated temperature of 700 °C were similar (in the case of S<sub>BET</sub>) or even superior (in the case of V<sub>mi</sub>

and V<sub>me</sub>) to the results obtained by other authors that used diverse fibers. These results imply a wide field of applications for these fibers.

#### References

- [1] Ahmadpour A, Do DD. The preparation of activated carbon from macadamia nutshell by chemical activation. Carbon 1997;35:1723-32.
- [2] Yoon SH, Korai Y, Mochida I, Carbon Fibers and Active Carbon Fibers, Science of Carbon Materials, H. Marsh, F. Rodríguez Reinoso (editors) Alicante, Publ. Universidad de Alicante, 2000.,
- [3] Rebouillat S, Peng JCM, Donnet J-B, Ryu S-K. Carbon Fiber Applications. In Donnet J-B, Wang TK, Rebouillat S, Peng JCM, editors. Carbon Fibers, New York: Marcel Dekker, 1998:463-541.
- [4] Tappi test method T203 om-93 (1994). Alpha-, beta-, and gamma- cellulose in pulp. Atlanta: Tappi press.
- [5] Tappi test method T236 om-85 (1994). Kappa number of pulp. Atlanta: Tappi press.
- [6] Valenzuela C, Bernalte A. Un método termogravimétrico rápido para el análisis inmediato de carbones. Boletín Geológico y Minero 1985;XCVI-I:58-61.
- [7] Brunauer S, Emmett PH, Teller E. Adsorption of gases in multi-molecular layers. J. Am. Chem. Soc. 1938;60:309-319
- [8] Dubinin M.M. Progress surface membrane science. In Danielli JF, Rosenberg MD, Cadenhead DA, editors. Vol. 9, New York: Academic Press, 1975: 1-14
- [9] Parr RG, Yang, Density-Functional Theory of Atoms and Molecules, Oxford University Press, Oxford, 1989.
- [10] Barrett EP, Joyner LG, Halena PP, The determination of pore volume and area distributions in porous substances. I. Computations from nitrogen isotherms. J. Am. Chem. Soc. 1951;73:373-380.
- [11] Stone J, Scallan A. The effect of component removal upon the porous structure of cell wall of Word. Pulp and paper magazine of Canada, 1968;6: 69-74.
- [12] Duchesne I, Daniel G. Changes in surface ultrastructure of Norway spruce fibers during kraft pulping- visualization by field emission SEM. Nordic pulp and paper research journal, 2000;15:54-61.
- [13] Keshk S, Suwinarti W, Sameshima K. Physicochemical characterization of different treatment sequences on kenaf bast fibers. Carbohydrate polymers, 2006;65: 202-206.
- [14] Mohd Eddeozey AM, Akil MD, Azhar B, Zainal Ariffin I. Chemical modification of kenaf fibers. Materials Letters, 2007;61:2023-2025.
- [15] Zaveri M. Absorbency characteristics of kenaf core particles. PhD North Carolina State University (2004).
- [16] Gaur V, Sharma A, Verma N. Preparation and characterization of ACF for the adsorption of BTX and SO<sub>2</sub>. Chemical Engineering and Processing. 2006;45: 1-13.
- [17] Ko T.H., Chiranairadul P, Lu CK, Lin CH. The effects of activation by carbon dioxide on the mechanical properties and structure of PAN-based activated carbon fibers. Carbon 1992;30:647-655.
- [18] Haiqin Rong, Zhenyu Ryu, Jingtang Zheng and Yuanli Zhang. Influence of heat treatment of rayon-based activated carbon fibers on the adsorption of formaldehyde. Colloid and Interface Science, 2003;26:207-212.
- [19] Suhas , P.J.M. Carrot, M.M.L. Ribeiro Carrot, Lignin- from natural adsorbent to activated carbon: A Review, Bioresource Technology, 2007;98:2305-2312.
- [20] Soo-Jin Park, Yu-Sin Jang, Jae Woon Shim and Seung-Kon Ryu. Studies on pore structures and surface functional groups of pith based activated carbon fibers. Journal of Colloid and Interface Science, 2003;26:259-264.

# Activated carbons as catalyst in the synthesis of fine chemicals

## Carbonos activados como catalizadores en la síntesis de productos de alto valor añadido

C. J. Durán-Valle<sup>1,2</sup>, R. C. Carvalho<sup>1</sup>, D. Omenat-Morán<sup>1</sup>, A. B. Botet-Jiménez<sup>1</sup>

<sup>1</sup> Departamento de Química Orgánica e Inorgánica.

<sup>2</sup> Instituto del Agua, Cambio Climático y Sostenibilidad. Universidad de Extremadura. Avda. de Elvas, s/n. 06006 Badajoz España

\*Corresponding autor: carlosdv@unex.es

### Abstract

The group of research *Sustainable and Environmental Chemistry*, part of the Extremadura System of Science and Technology, was established in 2006 bringing together researchers from various institutions in Extremadura related to research and innovation. Within its lines of work, dedication and most important results is the use of activated carbons (CAs) chemically modified as catalysts in the synthesis of fine chemicals (PAVs). In this paper, some of the most significant results obtained in this research are shown.

### Resumen

El grupo de investigación *Química Sostenible y Medioambiental*, perteneciente al Sistema Extremeño de Ciencia y Tecnología, se creó en el año 2006 reuniendo a investigadores de diversas instituciones extremeñas relacionadas con la investigación y la innovación. Dentro de sus líneas de trabajo, la más importante en dedicación y resultados es la utilización de carbonos activados (CAs) químicamente modificados como catalizadores en la síntesis de productos de alto valor añadido (PAVs). En este trabajo se muestran algunos de los resultados más significativos obtenidos en esta línea de investigación.

### 1. Introducción

Un gran número de procesos en la industria química se llevan a cabo mediante catálisis. El desarrollo de la Química Verde o Química Sostenible [1] ha impulsado la búsqueda de nuevos catalizadores más eficientes y menos agresivos con el medio ambiente. Un campo de interés para la aplicación de los catalizadores son los procesos de síntesis de PAVs [2], ya que por las circunstancias específicas de estas síntesis (moléculas complejas y poco estables, uso frecuente de disolventes orgánicos, procesos industriales no optimizados) la contaminación por unidad producida es mucho más elevada que en la fabricación de productos de química básica.

De los materiales que han captado el interés de los investigadores para su uso como catalizadores en los últimos años, destacan los CAs. Aunque el carbón se empleaba en la industria desde hace años [3], su uso se veía limitado por la falta de comprensión de sus propiedades, especialmente las químicas que son las que más influyen en su actividad catalítica. Pero el continuo estudio sobre estos materiales y la posibilidad de controlar la química superficial de los mismos han dado lugar [4] a un incremento importante del número de aplicaciones catalíticas de los CAs.

En esta línea, se muestran a continuación algunos

de los resultados más relevantes obtenidos en nuestro laboratorio acerca de la modificación química de carbonos activados y su utilización como catalizadores ácidos o básicos en la obtención de PAVs.

### 2. Catálisis ácida

Los carbonos activados pueden ser transformados en catalizadores ácidos por métodos sencillos y de coste limitado. Uno de esos métodos, comúnmente empleado, es la oxidación en presencia de agua. De esta manera, se favorece la formación de grupos oxigenados e hidrogenados como los carboxilos, que presentan propiedades ácidas. En nuestro grupo hemos preparado catalizadores empleando este método, tratando el carbón activado con ácido nítrico.

Otro método menos conocido pero que da lugar a catalizadores más efectivos es el tratamiento con ácido sulfúrico. Aunque este compuesto es ácido y oxidante como el ácido nítrico, su principal efecto en la preparación de catalizadores es que si se emplea en forma concentrada actúa además como sulfonante sobre los anillos aromáticos, creando grupos sulfónicos unidos covalentemente a las moléculas de grafeno. Estos grupos funcionales son ácidos mucho más fuertes que los grupos carboxílicos o sus derivados (Tabla 1), por lo que los catalizadores así obtenidos son más activos cuando se trata de reacciones catalizadas por ácidos.

Table 1.  $pK_a$  of some aromatic compounds.

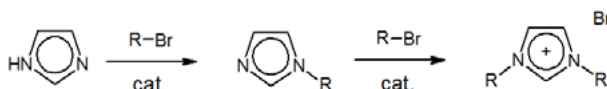
Tabla 1.  $pK_a$  de algunos compuestos aromáticos.

Compuesto	$pK_a$
Fenol	9.89
Ácido Benzoico	4.19
p-Nitrofenol	7.15
Ácido p-nitrobenzoico	3.41
Ácido bencenosulfónico	0.70

Los tratamientos con ácidos tienden a disminuir la superficie específica del carbón activado, aunque según nuestra experiencia no lo suficiente como para afectar a la actividad catalítica, mientras que esta capacidad sí que está fuertemente relacionada con la acidez del catalizador. El punto de carga cero (PCC) de estos materiales depende del carbón activado original y del ácido empleado, pero no del número de grupos funcionales ácidos existentes, demostrando que es más importante el tipo de grupo funcional que su número.

El material carbonoso tratado con ácido sulfúrico fue patentado para su uso como catalizador [5] en el año 2005, y desde entonces se ha ensayado en varias síntesis de PAVs.

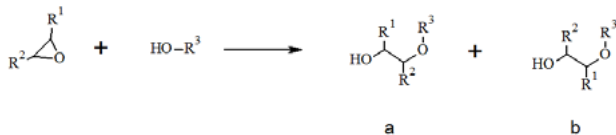
Una de estas reacciones ha sido la alquilación de heterociclos nitrogenados [6]. Esta reacción es útil para la obtención de fármacos antivirales, antibacterianos y antimicóticos, entre lo que hay algunos productos comerciales (Aciclovir, Miconazol, Ketoconazol, etc.). El objetivo inicial de la síntesis fue la monoalquilación del heterociclo, reacción que previamente se había ensayado en medio básico (ver el apartado 3) para obtener productos similares a los citados. Pero al emplear un catalizador ácido, especialmente si este es muy activo, encontramos que la reacción continuaba con una segunda alquilación, dando lugar a un líquido iónico (Esquema 1). Este es un tipo de compuestos que cada vez son más populares al emplearse como disolventes y catalizadores, entre otras aplicaciones.



**Scheme 1.** Reaction of imidazole with alkyl bromide.

**Esquema 1.** Reacción de imidazol con bromuro de alquilo.

Otra reacción ensayada fue la apertura del anillo de epóxido con alcoholes y aminas [7, 8, 9]. Es una reacción frecuentemente empleada en síntesis orgánica ya que permite la creación de centros quirales en la molécula. Generalmente se emplea en la obtención de compuestos intermedios en la síntesis de fármacos como antitumorales o inmunosupresores, pero los  $\beta$ -alcoxi-alcoholes obtenidos son también productos comerciales, ya que se usan como disolventes. Al emplear aminas, se obtienen  $\beta$ -aminoalcoholes, también de uso farmacológico. Esta reacción puede activarse con radiación MW [7,8]. Respecto a esta reacción hemos encontrado que la capacidad catalítica de estos carbonos aumenta con la acidez. Pero no es la única mejora obtenida. Un problema que se plantea en esta reacción es que se pueden producir dos aperturas distintas del anillo de epóxido, dando lugar a dos compuestos diferentes, según muestra el Esquema 2.



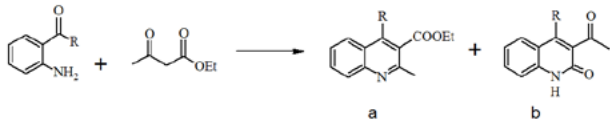
**Scheme 2.** Ring-epoxide opening with alcohol.

**Esquema 2.** Apertura de anillo de epóxido con alcohol.

Cuando se ha empleado un epóxido con un anillo cercano (alifático o aromático) se ha obtenido preferentemente la forma b del Esquema 2 con selectividades muy elevadas. En cambio, cuando el epóxido está unido a una cadena abierta (epoxy pentano o epoxy heptano), las selectividades no son elevadas y cualquiera de los dos compuestos puede ser el mayoritario. Hemos detectado que, de forma general, cuanto mayor es la acidez del catalizador, más elevada es también la selectividad de la reacción, y este efecto también se observa al aumentar la cantidad del catalizador.

La reacción de Friedländer consiste en la condensación de un compuesto 2-aminoaryl carbonílico con otro compuesto carbonílico para dar lugar a quinolinas (Esquema 3). Estas son una familia de compuestos que se emplean en medicina,

como aditivo alimentario, colorante, etc. La reacción se considera de elevada economía atómica, siendo este uno de los doce principios [1] de la Química Sostenible.



**Scheme 3.** Reaction of Friedländer between 2-aminoaryl ketone and ethyl acetoacetate.

**Esquema 3.** Reacción de Friedländer entre 2-aminoaryl cetona y acetoacetato de etilo.

Como en la reacción de apertura de epóxidos, se puede obtener una mezcla de productos, por lo que la selectividad del catalizador es de gran importancia en esta reacción. Esta selectividad puede mejorarse cambiando la estructura porosa o la acidez/basicidad del catalizador. Así, los catalizadores básicos dan lugar al compuesto b del Esquema 3, mientras que los catalizadores ácidos dan lugar a una mezcla de ambos compuestos. Por esta razón, es interesante aumentar la selectividad hacia el compuesto a de los catalizadores ácidos, ya que permitiría obtener uno u otro compuesto cambiando el tipo de catalizador.

Se estudiaron estos dos factores en un trabajo realizado con investigadores de la UNED y de la Universidad Nova de Lisboa [10]. La conversión obtenida al cabo de 4 horas a 363 K fue cercana al 100% al emplear 2-aminobenzofenona y acetoacetato de etilo, con una mejor selectividad para los carbonos microporosos y muy ácidos. Los resultados obtenidos son comparables o mejoran a los producidos por otros catalizadores como SBA sulfonado o la zeolita BEA, lo que demuestra que los carbonos activados pueden emplearse como catalizadores baratos y eficientes en la reacción de condensación de Friedländer. Una explicación a estos resultados puede obtenerse del estudio del estado de transición. Una simulación de la estructura por métodos de cálculo teóricos (utilizando el método B3LYP) indica que al emplear grupos sulfónicos, el estado de transición es más rígido que al emplear grupos ácidos carboxílicos. En este último caso, una mayor flexibilidad se traduce en un menor control de la selectividad.

Otra reacción ensayada con catalizadores ácidos es la obtención de acetales [11]. Estos son el producto de la reacción de una molécula de cetona con dos moléculas de alcohol.



**Scheme 4.** Synthesis of acetals.

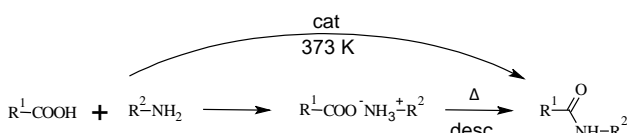
**Esquema 4.** Síntesis de acetales.

Esta reacción es ampliamente utilizada en síntesis orgánica para la protección de grupos carbonilo, ya que es fácilmente reversible. Los acetales, además, se emplean como fragancias, en productos farmacéuticos y como aditivos alimentarios. El rendimiento de esta reacción está limitado al producirse un equilibrio, y nosotros hemos obtenido entre el 25 y el 52% en función de los reactivos empleados, aunque con una selectividad muy elevada que generalmente supera el 95%. Pero al

ser un equilibrio, este se puede desplazar retirando del medio (o añadiendo en el caso de la reacción inversa) las moléculas de agua formadas en la reacción. Así, mediante destilación simultánea se consiguen rendimientos mayores, cercanos al 80% aunque necesitas tiempos más largos de reacción. Otro método para eliminar el agua formada es realizando el proceso en presencia de ortoformiato de alquilo. Este reacciona con agua para producir el alcohol correspondiente al alquilo empleado, y se alcanzan rendimientos elevados al emplear el catalizador con grupos sulfónicos, con una selectividad del 100 %, aunque también con tiempos de reacción más elevados.

Dos reacciones en la que se usan frecuentemente tanto la catálisis básica como la ácida son la esterificación y la transesterificación. En la primera, un ácido carboxílico reacciona con un alcohol para dar lugar a un éster. Es también un equilibrio, puesto que el éster se puede hidrolizar para rendir el ácido y alcohol correspondiente, lo que limita en muchos casos el rendimiento obtenido. En la transesterificación se parte de un éster que reacciona con un alcohol para dar lugar a otro éster diferente. De los carbones ácidos ensayados, nuevamente resulta ser el tratado con ácido sulfúrico [12] el más efectivo.

Una pareja de reacciones similares son la obtención de amidas y la transamidación. En el primer caso, se suele partir de un éster y no del ácido, ya que la reacción de éste con la amina da lugar a la sal de amonio del ácido, que debe descomponerse por pirolisis para dar la amida. Este proceso, utilizado frecuentemente en procesos industriales no es válido con PAVs, ya que estos suelen ser térmicamente inestables. Con nuestros catalizadores hemos conseguido obtener la amida directamente del ácido y la amina, sin necesidad de emplear temperaturas elevadas.



**Scheme 5.** Synthesis of amides.

**Esquema 5.** Síntesis de amidas.

En la Figura 1 se muestran los porcentajes de conversión al emplear un CA granular y una fibra de carbón activada, tanto en su forma original como después de ser tratados con ácido sulfúrico. Puede observarse que el tratamiento con el ácido es más efectivo en el CA granular.

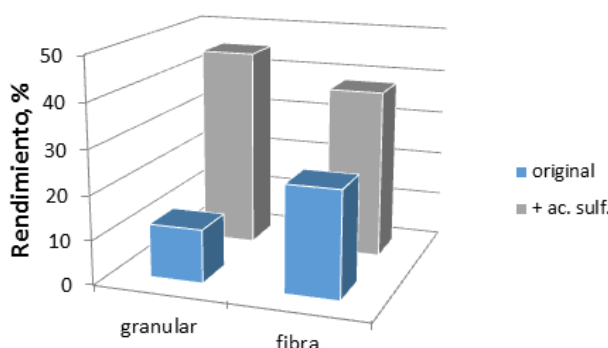
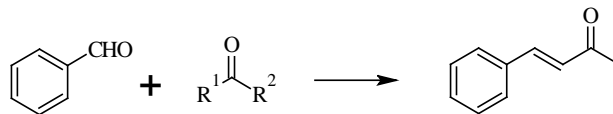


**Figure 1.** Yield in the reaction of acetic acid with hexylamine.

**Figura 1.** Rendimiento obtenido en la reacción de ácido acético con hexilamina.

La condensación de Claisen-Schmidt es la reacción entre un aldehído aromático y una cetona (Esquema 6). Se emplea un aldehído aromático ya que al no tener hidrógenos en posición alfa respecto al carbonilo, no puede dar lugar a la autocondensación, evitando la generación de productos no deseados. Se obtiene una cetona  $\alpha,\beta$ -insaturada, la cual podría volver a reaccionar con el aldehído, por lo que en este caso la selectividad del catalizador vuelve a ser tan importante como su capacidad de conversión.



**Scheme 6.** Claisen-Schmidt condensation.

**Esquema 6.** Condensación de Claisen-Schmidt.

El interés de esta reacción radica en que los compuestos obtenidos (denominados chalconas) poseen propiedades antibacterianas, antifúngicas, antitumorales y antiinflamatorias y además, son reactivos intermedios en la síntesis de flavonoides y flavonas, que también presentan actividad biológica.

Esta reacción habitualmente se cataliza con álcalis, y así se recoge en la mayoría de los libros de texto de química orgánica. Pero en nuestro laboratorio [13] hemos conseguido llevar a cabo esta reacción empleando un carbón sulfonado, de carácter ácido. Esto permite evitar ciertas reacciones colaterales que disminuirían la selectividad de la reacción. Los rendimientos obtenidos son elevados y además en todos los casos se ha observado un 100 % de selectividad. En la Figura 2 se muestran los resultados al emplear un xerogel de carbono. Al tratarlo con ácido sulfúrico (C-X-A-S) se obtiene un mayor rendimiento que al tratar el xerogel con ácido nítrico (C-X-N) o con sales de sodio (C-X-Na).

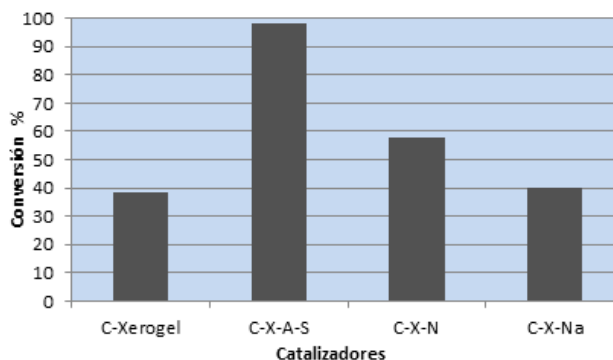


**Figure 2.** Synthesis of chalcone.

**Figura 2.** Síntesis de chalcona.

### 3. Catálisis básica

Los CA preparados por los métodos clásicos de carbonización y activación suelen tener un carácter alcalino, especialmente si la obtención se ha realizado en medio neutro o reductor. Esta característica ya permite que los materiales así preparados actúen como catalizadores, pero su capacidad como catalizadores puede mejorarse empleando varios métodos. Uno de ellos, que se ha ensayado en colaboración con el grupo *Catálisis no Convencional Aplicada a la Química Verde*, de la UNED, es la adsorción de cationes alcalinos (Na, K y Cs). Esta adsorción se realiza poniendo en contacto el carbón con una disolución de una sal del metal alcalino correspondiente.

Con este tratamiento, los carbones activados sufren una escasa variación en su estructura física, pero es más importante el cambio en las propiedades químicas. Así, cuanto más pesado es el elemento alcalino, mayor es la basicidad del catalizador, lo cual está relacionado directamente con su actividad catalítica.

Como ya se ha indicado en el apartado de catálisis ácida, una de las reacciones en las que más hemos trabajado es la alquilación de heterociclos nitrogenados. En medio básico no se obtienen líquidos iónicos, sino solamente el producto de la monoalquilación.

En algunos de los trabajos [14] se han empleado fuentes alternativas para suministrar energía a la reacción, como es la utilización de ultrasonidos (US). Así, en la reacción de 1-bromobutano con imidazol, para obtener N-butilimidazol (esquema 7) se puede observar que a todas las temperaturas ensayadas, los rendimientos mejoran al irradiar con ultrasonidos (Figura 3).

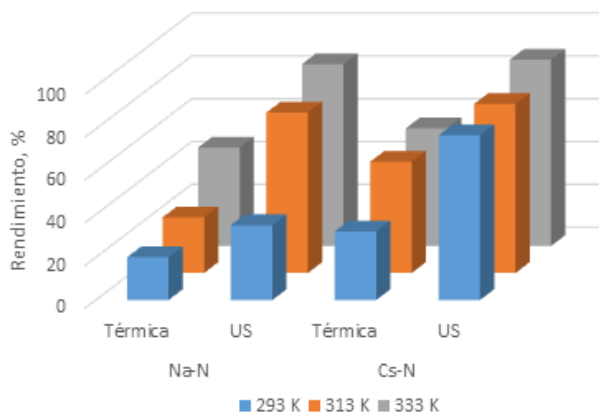
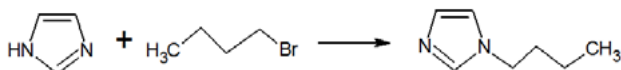


**Figure 3.** Yield in the synthesis of N-butylimidazole using alkaline activated carbon as catalysts.

**Figura 3.** Rendimiento en la obtención de N-butilimidazol empleando carbones activados alcalinos como catalizadores.

En esta figura se puede observar que el catalizador preparado con cesio es más activo que el preparado con sodio, lo cual sucede en todas las reacciones ensayadas. También hay que señalar que el efecto de la irradiación con ultrasonidos es más notable cuando los rendimientos son bajos, es decir, a baja temperatura y empleando el catalizador con sodio.



**Scheme 7.** Alkylation of imidazole with 1-bromobutane.

**Esquema 7.** Alquilación de imidazol con 1-bromobutano.

Otra reacción que se ha citado en el apartado de catálisis ácida y que también se ha realizado con catalizadores básicos es la condensación de Claisen-Schmidt. Se emplearon [15] dos carbones dopados con sodio y cesio, siendo este último el más activo ya que es el de mayor basicidad. Como en el caso anterior, la utilización de ultrasonidos mejora considerablemente el rendimiento de la reacción, manteniendo una selectividad cercana al 99%.

#### 4. Conclusiones

Es posible modificar por métodos sencillos y de bajo coste la estructura química de los carbones activados para mejorar sus propiedades como ácidos y álcalis.

Pueden actuar como catalizadores eficientes y de bajo coste, y de los resultados aquí mostrados se puede concluir que poseen un amplio espectro de aplicaciones en las síntesis de PAVs.

#### 5. Bibliografía

- [1] Anasta PT, Warner JC. *Green Chemistry: Theory and Practice*. Oxford University Press. 2000.
- [2] Sheldon RA, van Bekkum H. 1. Introduction. In: Sheldon RA and van Bekkum H, Eds. *Fine Chemicals through Heterogeneous Catalysis*. Ed. Wiley-VCH. 2001 p.1-11.
- [3] Rodríguez-Reinoso F. The role of carbon materials in heterogeneous catalysis. *Carbon*, 1998; 36:159-175.
- [4] Calvino-Casilda V, López-Peinado AJ, Durán-Valle CJ, Martín-Aranda RM. Last Decade of Research on Activated Carbons as Catalytic Support in Chemical Processes. *Catal Rev* 2010; 52:325-380.
- [5] Martín Aranda RM, Durán Valle CJ, Ferrera Escudero S. Patente española P200501605. 2005.
- [6] Durán-Valle CJ, Madrigal-Martínez M, Martínez-Gallego M, Fonseca IM, Matos I, Botelho do Rego AM. *Cat Today* 2012; 187:108-114.
- [7] García-Vidal JA, Durán-Valle CJ, Ferrera-Escudero S. Green chemistry: Efficient epoxides ring-opening with 1-butanol under microwave irradiation. *App Surf Sci* 2006; 252:6064–6066.
- [8] Durán-Valle CJ, García-Vidal JA. Acidic Activated Carbons: An Efficient Catalyst for the Epoxide Ring-Opening Reaction with Ethanol. *Catal Lett* 2009; 130:37–41.
- [9] Matos I, Neves PD, Castanheiro JE, Perez-Mayoral E, Martin-Aranda R, Duran-Valle C, Vital J, Botelho do Rego AM, Fonseca IM. Mesoporous carbon as an efficient catalyst for alcoholysis and aminolysis of epoxides. *Appl Catal A-Gen* 2012; 439-440:24-30.
- [10] López-Sanz J, Pérez-Mayoral E, Soriano E, Omenat-Morán D, Durán CJ, Martín-Aranda RM, Matos I; Fonseca I. Acid activated carbons: cheaper alternative catalysts for the synthesis of substituted quinolones. *ChemCatChem* 2013; 5:3736-374.
- [11] Durán Valle C, Pérez Mayoral E, Domínguez Fernández F, Botet Jiménez AB, Martínez Cañas MA, Omenat Morán D. Patente española P200902376. 2009.
- [12] Durán Valle CJ, Holguín Sánchez G, García Vidal JA, Madrigal Martínez M, Madrigal Martínez JR, Carmona Méndez J. Patente española P201030036. 2010.
- [13] Durán Valle CJ, Mora Díez N, Carvalho RC. Patente española P201131054. 2011.
- [14] Durán-Valle CJ, Ferrera-Escudero S, Calvino-Casilda V, Díaz-Terán J, Martín-Aranda RM. The effect of ultrasound on the catalytic activity of alkaline carbons: preparation of N-alkyl imidazoles. *Appl Surf Sci* 2004; 238:97-100.
- [15] Durán-Valle CJ, Fonseca I, Calvino-Casilda V, Picallo M, López-Peinado AJ, Martín-Aranda RM. Sonocatalysis and alkaline doped carbons: an efficient method for the synthesis of chalcones in heterogenous media. *Cat. Today* 2005; 107-108:500-506.

# Adsorption of phenol from aqueous solution by activated carbons derived from cherry stones

## Adsorción de fenol en disolución acuosa sobre carbonos activados obtenidos a partir de huesos de cereza

P.M. Álvarez<sup>1</sup>, J. Jaramillo<sup>1</sup>, V. Gómez-Serrano<sup>2</sup>

<sup>1</sup>Departamento de Ingeniería Química y Química Física, Universidad de Extremadura, Avda Elvas S/N, Badajoz, España.

<sup>2</sup>Departamento de Química Orgánica e Inorgánica, Universidad de Extremadura, Avda Elvas S/N, Badajoz, España.

\*Corresponding author: pmalvare@unex.es

### Resumen

En este trabajo se han preparado carbonos activados mediante activación física (con aire, dióxido de carbono y vapor de agua) a partir de huesos de cereza. Los carbonos activados se han caracterizado desde el punto de vista textural (adsorción de nitrógeno a 77 K y porosimetría de mercurio) y químico (grupos superficiales de oxígeno y punto de carga cero). Las muestras preparadas se han empleado para adsorber fenol en disolución, mostrando mayor capacidad de adsorción a medida que lo hace la superficie específica y microporosidad. No obstante, la adsorción química de fenol se vio favorecida por la presencia de grupos superficiales de oxígeno en el carbón. Los carbonos preparados con dióxido de carbono y vapor de agua mostraron una capacidad de adsorción de fenol comparable a la del carbón comercial Filtrasorb-400.

### Abstract

Samples of activated carbon were obtained by physical activation (air, carbon dioxide and steam as activating agents) of cherry stones. Activated carbon samples were characterized from the textural (nitrogen adsorption at 77 K and mercury porosimetry) and surface chemistry (surface oxygen groups and point of zero charge) points of view. Samples were used to adsorb phenol from aqueous solution, showing that phenol uptake was related to the surface area and microporosity. Nevertheless, chemisorption of phenol was favoured by surface oxygen groups. Samples activated in CO<sub>2</sub> and steam showed phenol adsorption capacities close to that of Filtrasorb-400, a well-known commercial activated carbon.

### 1. Introducción

La creciente demanda de carbón activado y las regulaciones medioambientales y de fomento del aprovechamiento de la biomasa han despertado un gran interés en el uso de residuos vegetales como precursores de carbonos activados [1]. Entre estos residuos, el hueso de cereza ha sido objeto de varios trabajos de investigación encaminados a la preparación de carbonos activados por diferentes métodos de activación física y química [e.g. 2-5]. En general, a partir de este material lignocelulósico se han obtenido carbonos activados que presentan alta superficie, microporosidad, bajo contenido en impurezas y una capacidad de adsorción, en algunos casos, comparable a la de carbonos activados comerciales [2,6].

La adsorción de fenol en carbón activado es uno de los procesos de adsorción en fase acuosa más

ampliamente estudiado. Así, es habitual referir la capacidad de adsorción de un carbón activado a la molécula de fenol (índice de adsorción de fenol). Otros compuestos fenólicos tales como fenoles sustituidos con halógenos, ácidos fenólicos, polifenoles, etc. también han sido objeto de numerosas investigaciones [7]. Así, en la bibliografía se pueden encontrar muchas publicaciones que reflejan la elevada afinidad que muestran diferentes carbonos activados, comerciales y preparados en el laboratorio, por compuestos fenólicos en fase acuosa. Sin embargo, a pesar de disponer de amplia información acerca del proceso de adsorción de fenol, el mecanismo específico por el que transcurre es bastante ambiguo [8]. En general, se acepta que la estructura porosa y la química superficial del carbón, la concentración y naturaleza del compuesto fenólico (solubilidad, pK<sub>a</sub>, grupos funcionales presentes, polaridad y tamaño molecular) así como el pH y la fuerza iónica de la disolución, juegan un papel fundamental sobre el modo en que transcurre la adsorción [9]. Además, se ha observado que la presencia o ausencia de oxígeno disuelto también afecta al mecanismo de adsorción [10]. Así, los compuestos fenólicos pueden adsorberse en carbón activado a través de la acción simultánea de mecanismos físicos y químicos, como los mostrados en la Figura 1 [11].

De acuerdo con la Figura 1, el fenol se puede adsorber: i) físicamente mediante interacciones hidrofóbicas (fuerzas de dispersión π-π) de forma reversible (A↔B); ii) mediante reacción química del fenol con grupos funcionales del carbón (A→C). El compuesto fenólico quimisorbido puede simplemente ocupar el centro de adsorción (C) o convertirse en un nuevo centro para la reacción de una nueva molécula de fenol (D). Las moléculas de fenol adsorbidas físicamente también pueden sufrir polimerización. Los polímeros productos de esta reacción pueden quedar retenidos físicamente en la estructura de poros del carbón activado (E), en cuyo caso pueden desorberse parcialmente hasta la fase acuosa (F), o permanecer quimisorbidos al carbón (G).

El objetivo de este trabajo es evaluar la capacidad para adsorber fenol de carbonos activados preparados a partir de hueso de cereza por métodos de activación física. Se estudia la influencia del método de activación y se discuten los mecanismos de adsorción física y química.

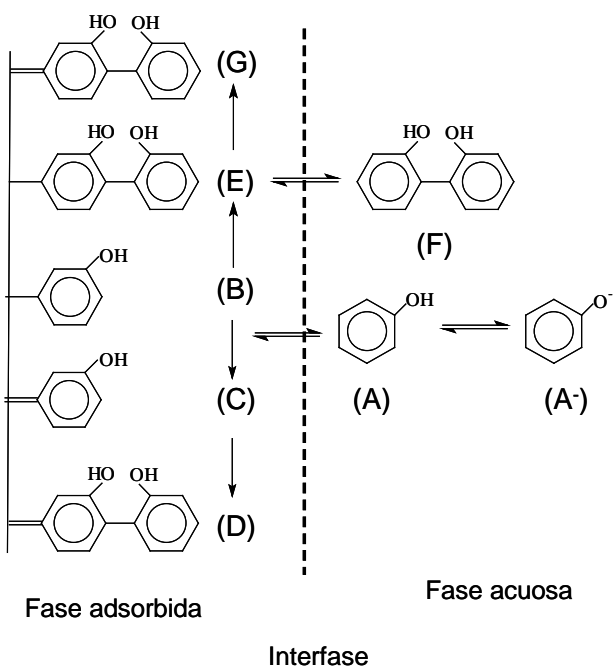


**Figura 1.** Diferentes mecanismos de adsorción de fenol en carbón activado.

**Figure 1.** Various mechanisms of phenol adsorption onto activated carbon.

## 2. Materiales y métodos experimentales

### 2.1 Preparación y caracterización de carbones activados

Los huesos de cereza utilizados en este trabajo fueron facilitados por la Agrupación de Cooperativas del Valle del Jerte (Valdeastillas, Cáceres). A su llegada al laboratorio, se procedió al lavado, secado, molienda y clasificación por tamaños de los mismos, seleccionando para este trabajo aquella fracción de tamaños comprendidos entre 1 y 2 mm. A partir de huesos de cereza, se prepararon muestras de carbón activado mediante activación física en dos etapas (carbonización en atmósfera de nitrógeno

seguida de gasificación en aire, dióxido de carbono o vapor de agua) y en una etapa (activación directa en vapor de agua). Las muestras de carbón activado preparadas fueron las indicadas en la Tabla 1.

Además de los carbones activados preparados a partir de huesos de cereza, en este trabajo se empleó el carbón activado comercial Filtrasorb 400 (Calgon Corp.) con fines comparativos.

La caracterización de la estructura porosa de los carbones activados se llevó a cabo empleando las técnicas de adsorción de nitrógeno a 77 K (Autosorb-1, Quantachrome) y porosimetría de mercurio (Autoscan-60, Quantachrome). Se emplearon los métodos BET y  $t$  para evaluar la superficie específica y el volumen de microporos. El volumen de mesoporos y macroporos se determinó a partir de los datos de intrusión de mercurio. La superficie química de las muestras de carbones activados se caracterizó mediante la determinación de grupos superficiales de oxígeno (GSO) ácidos y básicos y del punto de carga cero (PCZ) mediante los métodos de Boehm y Noh y Schawrz, respectivamente [12,13]. En la Tabla 2 se presentan los resultados de la caracterización de los carbones activados.

### 2.2 Isotermas de adsorción

Para obtener las isotermas de adsorción de fenol, se comenzaba pesando la cantidad adecuada de compuesto fenol con una precisión de 0,1 mg y se disolvía en agua ultrapura (Milli-Q, Millipore), previamente ajustada a pH 5 con  $\text{HNO}_3$ , hasta completar 1 L de disolución. A continuación, se disponían 20 mL de esta disolución en varios tubos de ensayo de vidrio de 30 mL de capacidad a los cuales se añadía una cantidad de carbón activado comprendida entre 0 y 500 mg. Los tubos se cerraban con su tapón roscado y se colocaban en gradillas situándose éstas en un baño termostático JP Selecta modelo Unitronic-Orbital, que se programaba a 25°C con una velocidad de agitación de 50 vaivenes/min. El control de la temperatura y agitación se mantenía

**Tabla 1.** Muestras de carbón activado preparadas a partir de hueso de cereza.

**Table 1.** Activated carbon samples derived from cherry stones

Muestra	T <sup>a</sup> carbonización	Agente activante	T <sup>a</sup> activación	Tiempo de activación
A-400-3	600°C	Aire	400°C	3 h
C-850-1	900°C	$\text{CO}_2$	850°C	1 h
C-850-2	900°C	$\text{CO}_2$	850°C	1 h
C-850-3	900°C	$\text{CO}_2$	850°C	1 h
H-850-3	900°C	Vapor de agua	850°C	3 h
H*-800-3	-	Vapor de agua	800°C	3 h

**Tabla 2.** Caracterización de los carbones activados usados en este trabajo.

**Table 2.** Characterisation of the activated carbon samples used in this work.

Muestra	S <sub>BET</sub> (m <sup>2</sup> /g)	V <sub>mi</sub> (cm <sup>3</sup> /g)	V <sub>me</sub> (cm <sup>3</sup> /g)	V <sub>ma</sub> (cm <sup>3</sup> /g)	GSO ácidos (μeq/g)	GSO básicos (μeq/g)	PCZ
A-400-3	508	0,231	0,038	0,285	171	158	5,7
C-850-1	386	0,187	0,049	0,305	124	347	8,1
C-850-2	604	0,299	0,055	0,341	138	385	8,8
C-850-3	731	0,347	0,075	0,406	156	420	9,1
H-850-3	901	0,383	0,134	0,473	92	369	9,8
H*-800-3	771	0,336	0,113	0,438	106	225	8,9
F-400	866	0,350	0,166	0,319	207	540	8,9

durante 7 días, tiempo suficiente para alcanzar el equilibrio de adsorción de fenol. Una vez transcurrido el tiempo de contacto programado, se reajustaba el pH y se tomaban muestras de cada tubo de ensayo y se filtraban a través de membranas filtrantes de 0,45 µm de tamaño de poro. Los filtrados se analizaban mediante espectrofotometría de absorción UV-visible. La concentración en la fase adsorbida se determinaba aplicando el siguiente balance de materia:

$$n_F = \frac{V}{M} (C_{0,F} - C_F) \quad (1)$$

donde  $n_F$  es la concentración de fenol en la fase adsorbida;  $V$  es el volumen de disolución;  $M$  es la masa de carbón activado empleada;  $C_{0,F}$  y  $C_F$  son las concentraciones inicial y final de fenol en la disolución.

### 2.3 Análisis de fenol en disolución

El análisis de la concentración de fenol en disolución acuosa se efectuó mediante espectrofotometría UV-visible en un equipo Spectronic Helios α utilizando cubetas de cuarzo de 1 cm de camino óptico y agua ultrapura como referencia. La longitud de onda de detección seleccionada fue de 270 nm. Se prepararon varias disoluciones acuosas patrón de fenol compuesto en el intervalo de concentraciones 0-100 mg/L, construyendo una recta de calibrado con el conjunto de medidas fotométricas. Las muestras acuosas a analizar se diluían con agua ultrapura empleando un factor de dilución adecuado para que la concentración resultante de fenol estuviese incluida en los márgenes de validez de las rectas de calibrado (0-100 mg/L). A continuación se efectuaba la medida de la absorbancia y se calculaba la concentración buscada teniendo en cuenta el coeficiente de absorbividad, el camino óptico (1 cm) y el factor de dilución.

### 2.4 Análisis de fenol adsorbido físicamente

Como se ha indicado anteriormente, la adsorción de fenol en carbón activado puede suceder por varios mecanismos. En general, cuando el mecanismo es de tipo físico, el fenol se desorbe térmicamente en un intervalo de temperaturas próximo a su temperatura de ebullición. Por otra parte, si el fenol se quimisorbe las fuerzas de adsorción son mayores por lo que se descompone en productos gaseosos a temperaturas notablemente más altas que la de ebullición [14]. Basándose en ello, es posible distinguir cuantitativamente entre las cantidades de fenol fisisorbido y quimisorbido en un carbón activado mediante análisis térmico. En la Figura 2 se muestran, a modo de ejemplo, los diagramas DTG obtenidos en el análisis térmico de un carbón activado virgen y saturado con fenol. En el termograma del carbón activado sin compuesto adsorbido se aprecian leves efectos térmicos asociables al desprendimiento de varios grupos superficiales de oxígeno. En el termograma del carbón saturado se observan picos más intensos debidos a la descomposición térmica del fenol adsorbido. El primer efecto térmico, assignable al material adsorbido físicamente, aparece a centrado a 150°C. El resto de efectos, que aparecen a mayor temperatura, son debidos principalmente a la descomposición del adsorbato quimisorbido.

En base a los resultados mostrados en la Figura 2, el análisis de fenol adsorbido físicamente se efectuaba en un equipo Mettler TA-3000 provisto de una termobalanza TG-50. El procedimiento analítico comenzaba pesando con precisión aproximadamente 100 mg de la muestra a analizar previamente secado en estufa a 80°C durante 24 h para retirar la humedad.

La muestra se introducía en el portamuestras de la termobalanza que previamente había sido calibrada. A continuación se hacía pasar un flujo de 200 mL/min de nitrógeno y se conectaba el sistema de calefacción programado para calentar a una velocidad de 10°C/min desde temperatura ambiente hasta 350°C. Al mismo tiempo se efectuaba un análisis, en las mismas condiciones, con una muestra de carbón activado virgen (sin compuesto fenólico adsorbido). Una vez registrados los termogramas, se integraba el pico de la curva DTG correspondiente al primer efecto térmico del análisis del carbón saturado y se restaba el área bajo la curva del ensayo en blanco (carbón sin compuesto adsorbido), estimándose así la masa de compuesto fenólico que se encontraba adsorbido físicamente en el carbón,  $m_F$ . Si  $m$  (mg) es la masa de muestra empleada en el análisis y  $n_i$  (mg/g) la cantidad de fenol adsorbido por gramo de carbón, las concentraciones de fenol adsorbido físicamente,  $n_{Fi}$  (mg/g), y químicamente,  $n_{Qi}$  (mg/g), se pueden calcular mediante las expresiones (2) y (3):

$$n_{Fi} = \frac{m_F \cdot (1+n_i)}{m} \quad (2)$$

$$n_{Qi} = n_i - n_{Fi} \quad (3)$$

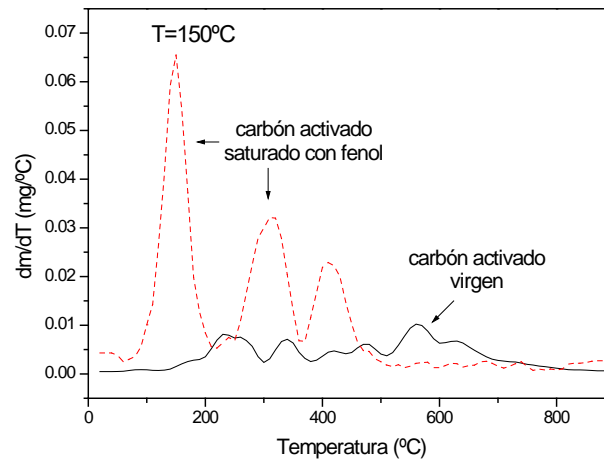


**Figura 2.** Diagramas DTG de muestras de un carbón activado virgen y saturado con fenol

**Figure 2.** DTG plots of virgin and phenol loaded activated carbon samples.

### 3. Resultados y discusión

El objetivo de este estudio es conocer la capacidad de adsorción de los carbones preparados a partir de hueso de cereza. La discusión de resultados acerca de la capacidad de adsorción se ha efectuado bajo un criterio de comparación con la que presenta el carbón activado comercial Filtrasorb 400 (F-400). Se trata de un carbón activado granular con un tamaño de partícula medio de 1 mm, fabricado a partir de carbón bituminoso mediante activación física empleando

vapor de agua. Es un material de uso muy difundido en la eliminación de contaminantes del agua tales como sustancias húmicas, pesticidas y compuestos fenólicos. En un trabajo previo [15] se han obtenido las isotermas de adsorción de fenol sobre F-400 observándose que se ajustan con bastante precisión al modelo de adsorción de Freundlich:

$$n_e = K_F \cdot C_e^n \quad (4)$$

donde  $n_e$  y  $C_e$  son las concentraciones en equilibrio en la fase sólida y líquida, respectivamente y  $K_F$  y  $n$  son las constantes del modelo. Para éstas se encontraron valores de  $K_F=245$  (mg/g)·(L/mg)<sup>0,344</sup> y  $n=0,344$  [15].

El índice de adsorción de fenol, relativo al carbón activado F-400,  $IA_F$ , se ha definido mediante la expresión (5):

$$IA_F = \frac{100}{NP} \sum_{j=1}^{NP} \frac{n_j}{\left[ K_F \cdot C_j^n \right]_{F400}} \quad (5)$$

donde  $NP$  es el número de datos que definen la isoterma de adsorción de fenol en el carbón activado;  $C_j$  y  $n_j$  la concentración de fenol en disolución y adsorbida para cada dato de equilibrio  $j$ ; y  $K_F$  y  $n$  los parámetros del modelo de Freundlich para la adsorción de fenol en el carbón activado F-400. De esta manera, el carbón empleado como referencia (F-400) tendrá un índice de adsorción de fenol de 100.

En la Figura 3 se presentan gráficamente las isotermas de adsorción de fenol a 25°C y pH 5 en carbones activados preparados mediante diferentes métodos de activación. Se puede observar que todas las curvas isotermas responden a la tipología L de Giles y favorable de Manes y Hofer. También a simple vista, por la posición relativa de las curvas isotermas, se deduce que la capacidad de adsorción sigue el orden creciente siguiente: A-400-3 < C-850-3 < H\*-800-3 < H-850-3. Es decir, los carbones activados con

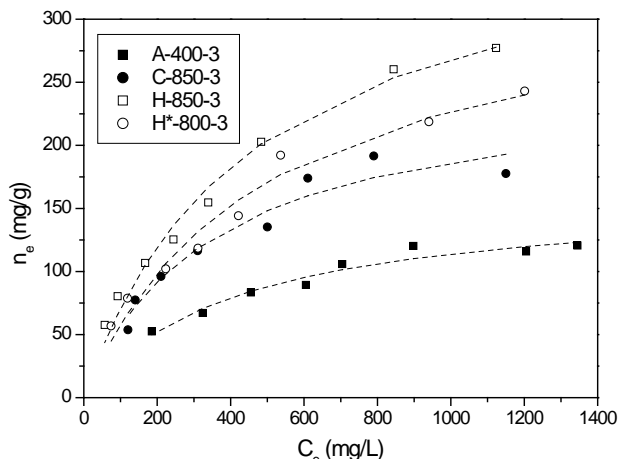


**Figura 3.** Isotermas de adsorción de fenol a 25°C y pH 5 en varios carbones activados preparados a partir de hueso de cereza por activación física con aire (A-400-3), dióxido de carbono (C-850-3) y vapor de agua (H-850-3 y H\*-800-3).

**Figure 3.** Phenol adsorption isotherms at 25°C and pH 5 of some activated carbon samples prepared from cherry stones by physical activation in air (A-400-3), carbon dioxide (C-850-3) and steam (H-850-3 y H\*-800-3).

vapor de agua son los mejores para adsorber fenol. Este resultado es, en principio, lógico atendiendo a las superficies específicas de los materiales.

Si se compara la capacidad de adsorción de los carbones activados preparados a partir de hueso de cereza con la de F-400, por aplicación de la ecuación (5) se obtienen los siguientes índices: 44,4 (A-400-3) < 69,3 (C-850-3) < 78,4 (H\*-800-3) < 90,1 (H-850-3). De acuerdo con ello, se puede decir que, empleando vapor de agua como agente activante, es posible preparar, a partir de hueso de cereza, carbones activados con una capacidad adsorbente (hacia el fenol) algo inferior, pero próxima, a la del producto comercial.

Para examinar si la adsorción de fenol ocurría principalmente por mecanismos físicos o químicos se obtuvieron las isotermas de fisisorción y quimisorción de fenol para los carbones C-850-3 y H-850-3 (Figura 4).

Los resultados de la Figura 4 muestran claramente que la fisisorción es dominante en el carbón activado H-850-3, mientras que en el carbón C-850-3 el fenol se retiene en la superficie mayoritariamente a través de enlaces químicos. Estos resultados conducen a pensar que la química superficial de los carbones activados juega un papel muy importante en el proceso de adsorción de fenol. Según puede verse en la Tabla 2, el carbón activado preparado con vapor de agua (H-850-3) posee una concentración de GSO, tanto ácidos como básicos, bastante más baja que el carbón activado en dióxido de carbono (C-850-3). Los grupos ácidos, por una parte, debilitan las fuerzas de dispersión por localización de los electrones de los anillos aromáticos de la capa de grafeno [16]. Por otra, pueden verse implicados en varios mecanismos de reacción con el fenol tales como enlaces de hidrógeno con el grupo OH del fenol [17] o formación de complejos dador-aceptor [18]. En cuanto a ciertos GSO básicos (estructuras tipo pirona y cromeno), parecen ser los principales catalizadores de la adsorción irreversible por oxidación con oxígeno y polimerización del fenol en la superficie del carbón [10]. En relación con

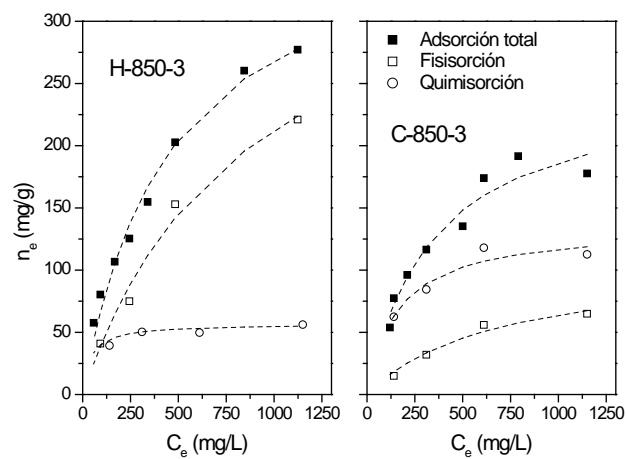


**Figura 4.** Isotermas de adsorción total, adsorción física y adsorción química de fenol a 25°C y pH 5 en los carbones activados H-850-3 y C-850-3.

**Figure 4.** Phenol adsorption (total, physical adsorption and chemical adsorption) isotherms at 25°C and pH 5 on activated carbons H-850-3 y C-850-3.

esto último, es interesante mencionar que en las disoluciones de fenol en contacto con los carbones H-850-3 y C-850-3, especialmente con el último, mostraban coloración marrón tras varios días de contacto en el baño isotérmico. Aunque no se realizó la identificación de los productos, la coloración es con toda seguridad debida a productos poliméricos que no quedan retenidos en el carbón, según se ha esquematizado en la Figura 1.

#### 4. Conclusiones

Los carbones activados preparados en este trabajo mediante activación física, en una o dos etapas, de huesos de cereza tienen unas propiedades texturales y una capacidad de adsorción de fenol comparables a las del carbón activado comercial Filtrasorb-400. De los métodos de activación empleados aquellos en los que se empleó vapor de agua como agente activante dieron lugar a los carbones activados con una superficie porosa más desarrollada y mayor capacidad para adsorber fenol físicamente. Por otra parte, la muestra de carbón activado preparada con dióxido de carbono tiene una superficie química con una mayor concentración de grupos superficiales de oxígeno que favorecen la químisorción de fenol.

#### 5. Agradecimientos

Los autores agradecen a la Junta de Extremadura la financiación de este trabajo a través del proyecto PDT08-A012.

#### 6. Bibliografía

- [<sup>1</sup>] Yahya MA, Al-Qodah Z. Agricultural bio-waste materials as potential sustainable precursors used for activated carbon production: A review. *Renew. Sust. Energ. Rev.* 2015; 46: 218-235.
- [<sup>2</sup>] Lussier MG, Shull JC, Mille, DJ. Activated carbon from cherry stones. *Carbon.* 1994; 32(8): 1493-1498.
- [<sup>3</sup>] Olivares-Marín M , Fernández-González C, Macías-García A, Gómez-Serrano V. Preparation of activated carbon from cherry stones by chemical activation with  $ZnCl_2$ . *Appl. Surf. Sci.* 2006; 252(17):5967-5971.
- [<sup>4</sup>] Olivares-Marín M, Fernández-González C, Macías-García A, Gómez-Serrano V. Porous structure of activated carbon prepared from cherry stones by chemical activation with phosphoric acid. *Energ. Fuel.* 2007; 21(5): 2942-2949.
- [<sup>5</sup>] Nowicki P, Kazmierczak J, Pietrzak R. Comparison of physicochemical and sorption properties of activated carbons prepared by physical and chemical activation of cherry stones. *Powder Technol.* 2014; 269: 312-319
- [<sup>6</sup>] Beker U, Ganbold B, Dertli H. Adsorption of phenol by activated carbon: Influence of activation methods and solution pH. *Energy Convers. Manage.* 2010; 51(2):235-240.
- [<sup>7</sup>] Dąbrowski A, Podkościelny P, Hubicki Z, Barczak M. Adsorption of phenolic compounds by activated carbon - A critical review. *Chemosphere.* 2005; 58(8):1049-1070.
- [<sup>8</sup>] Terzyk AP. Further insights into the role of carbon surface functionalities in the mechanism of phenol adsorption. *J. Colloid Interf. Sci.* 2003; 268(2):301-329.
- [<sup>9</sup>] Haghseresht F, Nouri S, Finnerty JJ, Lu GQ. Effects of surface chemistry on aromatic compound adsorption from dilute aqueous solutions by activated carbon. *J. Phys. Chem. B.* 2002; 106(42):10935-10943
- [<sup>10</sup>] Yan L, Deeter V, Lalley J, Medellin O, Kupferle MJ, Sorial GA. Effects of oligomerization phenomenon on dissolved organic matter removal kinetics on novel activated carbons. *J. Hazard. Mat.* 2014; 278(15):514-519
- [<sup>11</sup>] De Oliveira Pimenta AC, Kilduff JE. Oxidative coupling and the irreversible adsorption of phenol by graphite. *J. Colloid Interf. Sci.* 2006; 293(2):278-289.
- [<sup>12</sup>] Boehm HP. Some aspects of the surface chemistry of carbon blacks and other carbons. *Carbon.* 1994; 32(5):759-769.
- [<sup>13</sup>] Noh JS, Schwarz JA. Estimation of the point of zero charge of simple oxides by mass titration. *J. Colloid Interf. Sci.* 1989; 130(1):157-164
- [<sup>14</sup>] Moreno-Castilla C., Rivera-Utrilla J, Joly JP, López-Ramón MV, Ferro-García MA, Carrasco-Marín F. Thermal regeneration of an activated carbon exhausted with different substituted phenols. *Carbon.* 1995; 33(10):1417-1423.
- [<sup>15</sup>] Álvarez et al., 2005 Álvarez PM, García-Araya JF, Beltrán FJ, Masa FJ, Medina F. Ozonation of activated carbons: Effect on the adsorption of selected phenolic compounds from aqueous solutions. *J. Colloid Interf. Sci.* 2005; 283(2):503-512.
- [<sup>16</sup>] Salame II, Bandosz TJ. Role of surface chemistry in adsorption of phenol on activated carbons. *J. Colloid. Interf. Sci.* 2003; 264(2):307-312.
- [<sup>17</sup>] Franz M, Arafat HA, Pinto NG. Effect of chemical surface heterogeneity on the adsorption mechanism of dissolved aromatics on activated carbon. *Carbon.* 2000; 38(13):1807-1819.
- [<sup>18</sup>] Mattson JS, Mark HB, Malbin MD, Weber WJ, Crittenden JC. Surface chemistry of active carbon: specific adsorption of phenols. *J. Colloids Intef. Sci.* 1969; 31(1):116-130.

# Activated carbons developed in different activation conditions to improve nitrate adsorption performance

S. Román<sup>1\*</sup>, B. Ledesma<sup>1</sup>, M. E. Fernandez<sup>2,3,4</sup>, G. V. Nunell<sup>2,3,4</sup>, P. R. Bonelli<sup>2,3,4</sup>, A. L. Cukierman<sup>2,3,4</sup>

<sup>1</sup> Dpto. Física Aplicada, Universidad de Extremadura, Avda. Elvas s/n, 06006, Badajoz, Spain.

<sup>2</sup> Universidad de Buenos Aires, Facultad de Ciencias Exactas y Naturales, Departamento de Industrias, Programa de Investigación y Desarrollo de Fuentes Alternativas de Materias Primas y Energía-PINMATE, Intendente Güiraldes 2620, Ciudad Universitaria, (C1428BGA) Buenos Aires, Argentina.

<sup>3</sup> Consejo Nacional de Investigaciones Científicas y Técnicas (CONICET), Godoy Cruz 2290 (C1425FQB), Buenos Aires, Argentina.

<sup>4</sup> Universidad de Buenos Aires, Facultad de Farmacia y Bioquímica, Departamento de Tecnología Farmacéutica, Cátedra de Farmacotecnia II, Junín 956, (C1113AAD) Buenos Aires, Argentina

\* sroman@unex.es, Tel: +34924289600, Fax: +34924289601

## Abstract

The suitability of activated carbons (ACs) with dissimilar textural and surface chemistry characteristics was studied for nitrate removal, under different pH conditions. For this task, four ACs were used; two of them were manufactured by chemical and physical steam activation from orange peel and almond shell, while the other two were commercial adsorbents. It was found that both the precursor and activation methodology influence the adsorbents characteristics. Regarding nitrate uptake, their chemical surface was very relevant, while the textural properties did not exert a remarkable effect. Also, nitrate adsorption under acid pH was improved, especially for basic adsorbents, in contrast with neutral conditions, in which case no adsorbent stood out. The amelioration of nitrate removal for basic adsorbents and acidic pH conditions was associated to a greater prominence of electrostatic contributions as well as a lower extent of adsorption competition between hydroxyl and nitrate ions.

## Resumen

La idoneidad de carbonos activados (CAs) con características texturales y de química superficial diferentes se estudió para la eliminación de nitratos bajo diferentes condiciones de pH. Para ello se utilizaron cuatro CAs; dos de ellos comerciales y otros dos manufacturados mediante activación química y física a partir de cáscara de naranja y de almendra, respectivamente. Los resultados obtenidos mostraron que el precursor y la metodología de activación influyen en las características adsorbentes. En cuanto a la capacidad de adsorción, su superficie química fue muy relevante, mientras que las propiedades texturales no ejercieron un efecto notable. Además, la adsorción de nitrato mejoró a pH ácido, especialmente en el caso de los adsorbentes básicos, lo cual se asoció a una mayor importancia de las contribuciones electrostáticas así como, una menor adsorción competitiva entre los iones hidroxilo y nitrato.

## 1. Introduction

The discharge of nitrogen compounds to the environment has become a major question of concern, due to their severe effects on living species and ecosystems. In the particular case of nitrate compounds ( $\text{NO}_3^-$ ), due to its high water solubility, they are considered one of the most widespread groundwater contaminants in the

world, imposing a serious threat to drinking water supplies and promoting eutrophication [1-2]. High nitrate concentrations in surface and ground water reservoirs are mostly related to agricultural activities; precipitation, irrigation, and sandy soils allow nitrates to move around and find its way into surface water and groundwater [3]. Consumption of water with nitrates can lead to the formation of carcinogenic compounds such as nitrosamine, and also causes an increase in the rate of formation of methemoglobin in the blood, decreasing its oxygen-carrying capacity and leading to tissue hypoxia [4].

Among the several ways for nitrate removal, adsorption onto Activated Carbons (ACs) is an attractive option due to its simplicity and low cost, also because it usually does not require additional post-treatments and does not involve the generation of additional by-products [1].

The presence of heteroatoms on ACs surfaces has a significant effect on the chemical character, acidity and degree of hydrophobicity of its surface and hence plays a significant role on the adsorption performance of these materials. Some previous works have already pointed out that the surface chemistry of the adsorbent have a significant influence onto its nitrate adsorption behaviour. For example, Ota et al. [5] found that nitrate adsorption was almost negligible onto acidic ACs, while it was enhanced after the adsorbents had been outgassed at high temperatures (800-1000 °C), due to the elimination of oxygen surface groups. Afkhami et al. [6] studied the adsorption of nitrates onto activated cloths chemically modified with  $\text{H}_2\text{SO}_4$  and found that acid adsorbents yielded greater adsorption nitrate capacities; they concluded that acidic treatments protonated surface groups, enhancing electrostatic adsorption of ions, at the working pH.

Although the convenience of optimizing the ACs surface chemistry rather than its porous structure for this particular application has been confirmed, all of the assays were made without any adjustment of the solution pH, despite its great influence on nitrate adsorption performance.

The very few works on nitrate adsorption systems under different pH conditions have given evidence about the important role of this parameter, which can modify the adsorption mechanism, due to the enhancement of electrostatic contributions, in such a way that the trend can be totally inverted. For example, Nunell et al. [10] investigated the

adsorption of nitrates on ACs under different pH conditions and found that decreasing pH gave rise to an improvement in its nitrate uptake, since it promoted the adsorbent surface protonation. The variety of results found in the bibliography, as well as the lack of unified experimental conditions makes the understanding of the mechanisms governing nitrate adsorption very difficult, and demonstrates the need of studying each particular system.

On the other hand, both physical and chemical characteristics of ACs depend on the precursor used and the activation process applied for its preparation. With the motivation of searching new precursors, this work studied the production of ACs from orange peel (OP) and almond shells (AS), by chemical and physical activation, respectively, and their use as nitrate adsorbents. Adsorption was also studied on two commercial ACs (COM1 and COM2), to provide a variety of porosity and surface chemistry features.

## 2. Experimental

### 2.1. Precursors

Both commercial (COM1, *Chemviron Carbon*, from coconut shell, COM2, *Sigma Aldrich*, from bituminous coal) and home-made ACs were used. In the case of prepared adsorbents, almond shells (Extremadura, Spain) and orange peel (Buenos Aires, Argentina) were used as precursors.

### 2.2. Preparation of Activated Carbons

The ACs were produced from OP and AS by chemical and physical activation, respectively. Chemical activation was carried out according to the procedure described elsewhere [8]. Physical activation was made according to the procedure described in ref. [9], using an AS char previously obtained by pyrolysis (873 K, 1 h). Activation of the char was made with steam ( $0.10 \text{ g min}^{-1}$ ) diluted in nitrogen ( $100 \text{ mL min}^{-1}$ ) during 60 min, at 1123 K.

### 2.3. Characterization of activated carbons

#### 2.3.1. Textural characterization

ACs were characterized by means of  $\text{N}_2$  and  $\text{CO}_2$  adsorption at 77 K and 273 K, respectively (Micromeritics ASAP 2020 HV). Nitrogen adsorption data were used to calculate typical textural parameters by means of suitable models [10].

The surface morphology of the adsorbents was

examined by Scanning Electron Microscopy (SEM, Quanta 3D FEG, FEI). The sample was prepared by depositing about 50 mg on an aluminum stud covered with conductive adhesive carbon tapes, and then coating with Rh-Pd for 1 min to prevent charging during observations. Imaging was done in the high vacuum mode at an accelerating voltage of 30 kV, using secondary electrons under high vacuum conditions.

### 2.3.2. Chemical characterization

The total amounts of acidic/polar oxygen functional groups on the surface of the adsorbents ( $m_{\text{eq}}$  per gram of AC) was determined following a modified procedure based on Boehm's method. Also, the content of basic surface groups ( $m_{\text{eq}}$  per gram of AC) was determined by contacting 0.5 g of each AC with 50 mL of 0.05 mol L<sup>-1</sup> acid solutions. Subsequently, the slurries were stirred for 24 h and filtered. Afterwards, a 10 mL aliquot of the solutions was titrated with 0.05 mol L<sup>-1</sup> NaOH. Finally, the point of zero charge (PZC) of the adsorbents was determined following the procedure described by Carrot et al. [11].

### 2.3. Determination of adsorption isotherms

Nitrate adsorption isotherms were determined on the basis of batch analysis; a fixed mass of adsorbent was allowed to equilibrate with solutions of ions of known initial concentrations. Isotherms were made with different pH conditions: a) neutral pH, b) pH=2 with no addition of buffer, and c) pH=2 with the addition of buffer (HCl and KCl). In all cases, a stock sodium nitrate solution (16.1 mmol L<sup>-1</sup>) was firstly prepared, and from it, standard solutions of concentrations in the range 0.05-8.00 mmol L<sup>-1</sup> were obtained. Nitrate concentration was determined by UV-Vis spectrophotometry (Shimadzu UV mini-1240 analyzer) at 201 nm, obtaining a calibration correlation coefficient higher than 0.999.

## 3. Results and discussion

### 3.1. Characterization of Activated Carbons

Figure 1.a displays  $\text{N}_2$  adsorption isotherms at 77 K. From the plots it is evident that the adsorbents differ in both their  $\text{N}_2$  adsorption capacity and the porosity type.

While COM1 and CAS exhibit a type-I isotherm, denoting their microporous nature, COM2 and COP adsorption data depict a gradual increase of

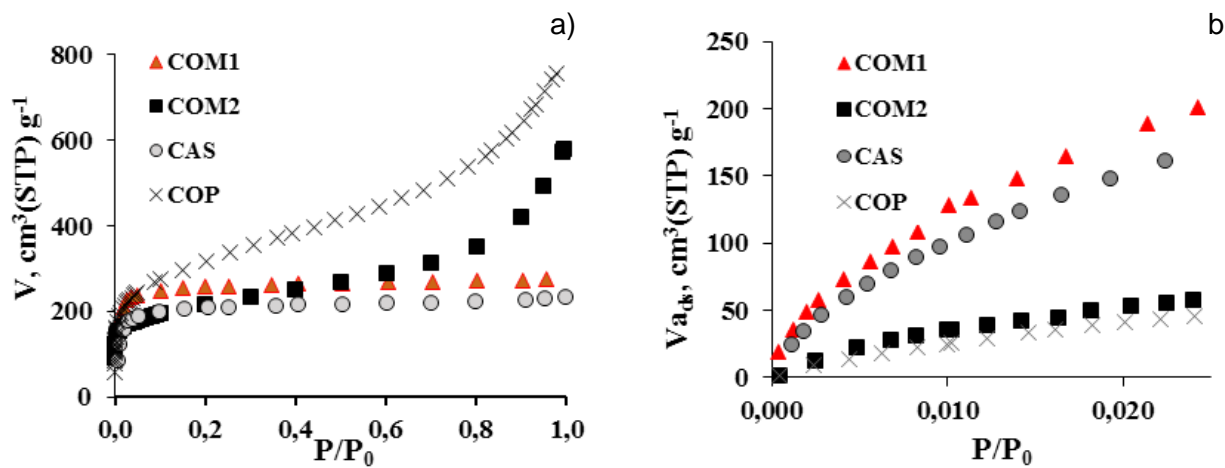


Figure 1.  $\text{N}_2$  (a) and  $\text{CO}_2$  (b) adsorption isotherms at -196 and 0 °C, respectively.

Figura 1. Isotermas de adsorción de  $\text{N}_2$  (a) y  $\text{CO}_2$  (b) a -196 y 0 °C, respectivamente.

**Table 1.** Textural parameters as derived from N<sub>2</sub> and CO<sub>2</sub> adsorption data.**Tabla 1.** Parámetros texturales derivados de los datos de adsorción de N<sub>2</sub> y CO<sub>2</sub>

	S <sub>BET</sub> [m <sup>2</sup> g <sup>-1</sup> ]	V <sub>miN<sub>2</sub></sub> [cm <sup>3</sup> g <sup>-1</sup> ]	V <sub>me</sub> [cm <sup>3</sup> g <sup>-1</sup> ]	S <sub>EXT</sub> [m <sup>2</sup> g <sup>-1</sup> ]	%S <sub>int</sub> [m <sup>2</sup> g <sup>-1</sup> ]	V <sub>micO<sub>2</sub></sub> [cm <sup>3</sup> g <sup>-1</sup> ]
<b>COM1</b>	857	0.413	0.010	25	97	0.717
<b>COM2</b>	710	0.310	0.254	119	83	0.253
<b>CAS</b>	641	0.340	0.011	29	96	0.616
<b>COP</b>	1090	0.298	0.758	540	50	0.217

adsorbed volume up to high relative pressure values, which suggest their mesoporous character. Besides, from Fig. 1, as well as from the textural parameters obtained from N<sub>2</sub> adsorption data, collected in Table 1, it can be observed that COP had the highest value of BET surface while CAS had the lowest.

This information can also be deduced from CO<sub>2</sub> adsorption isotherms (see Fig. 1.b), which show a greater adsorption for these two ACs, indicating a higher volume of primary micropores.

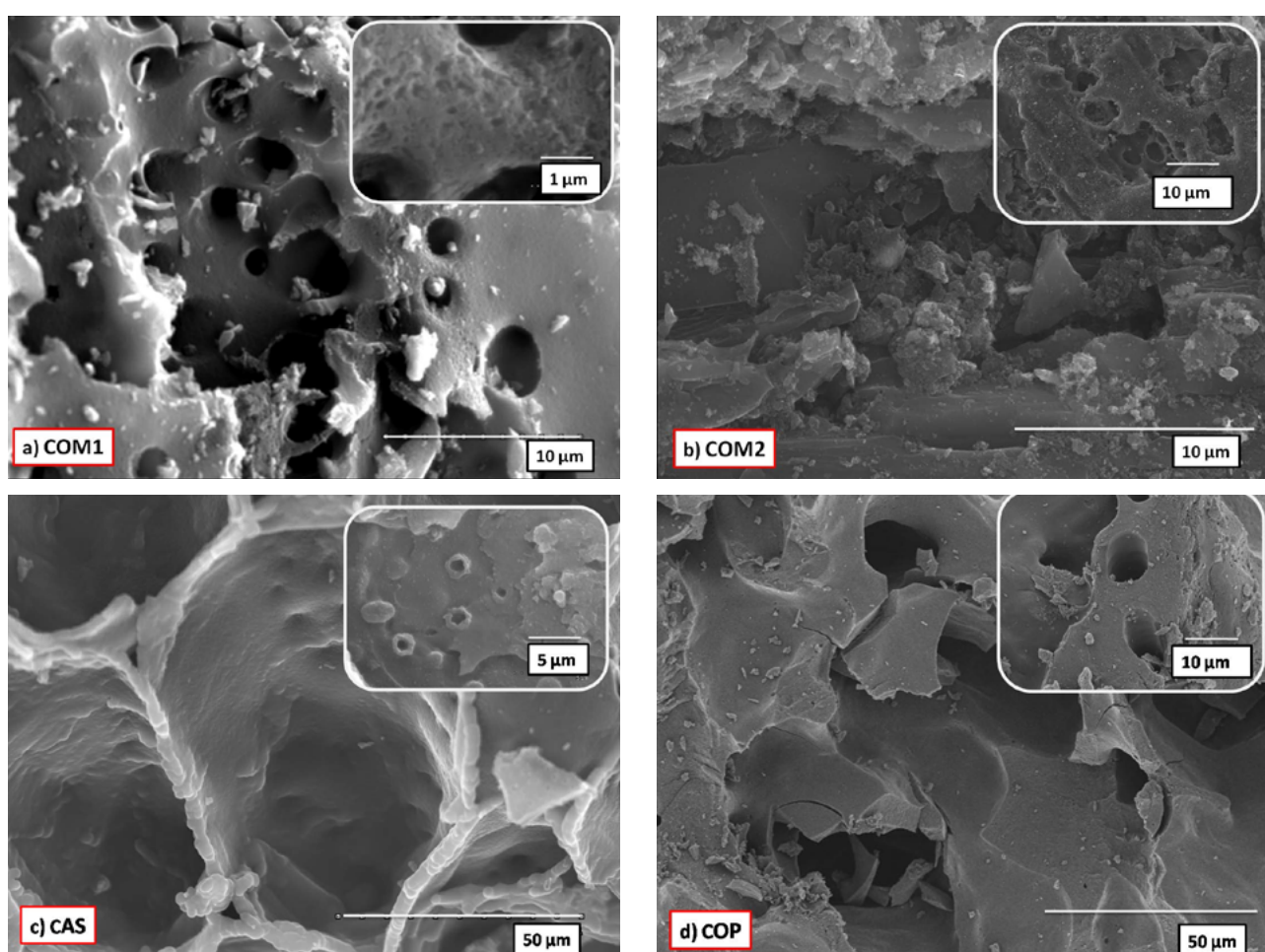
The comparison of N<sub>2</sub> and CO<sub>2</sub> as has been traditionally regarded as a powerful tool in order to improve the characterization of the smallest porosity, since the former gas can not get access to these pores under the working temperature; in this way, if V<sub>miN<sub>2</sub></sub><V<sub>micO<sub>2</sub></sub>, it is assumed that the solid has predominance of ultramicropores, while if the opposite occurs, then the solid is more likely to have large micropores and mesopores [12]. From Table 1, where the values of micropore volumes as determined from application of DR method to CO<sub>2</sub> adsorption data are presented, the predominance of ultramicropores for samples

COM1 and CAS can be confirmed.

It is remarkable that the difference between V<sub>micO<sub>2</sub></sub> and V<sub>miN<sub>2</sub></sub> is largest for COM1, denoting its important contribution of ultramicropores. A detailed inspection of N<sub>2</sub> adsorption isotherms reveals that the knee of the curve at lower P/P<sub>0</sub> is very abrupt, in coherence with this fact.

Figure 3 (a-d) displays the SEM micrographs made for the adsorbents at different magnifications. In general, all the samples present white particles on the surface, which can be attributed to sintering of the precursor inorganic matter during the heating treatment; these particles become more clearly visible for samples COM1 and COM2.

Besides, it is evident that the differences on the precursor as well as the processing methodology influence the surface appearance of adsorbent. For example, carbon COM1 (Fig. 3a) stands out due to their cylindrical pores, while COM2 (Fig. 3.b) is composed of macrometer-sized monolithic fragments with sharp edges. Regarding the manufactured ACs

**Figure 3.** SEM micrographs of ACs. Lower size image: magnification of 10000; larger image: magnification of 2000.**Figura 3.** Micrografías SEM de CAs. Imagen de menor tamaño: aumento de 1000; mayor tamaño: aumento de 2000.

(Fig. 3c and d), the pores resemble the cell walls of the original plant structures, exhibiting great opened cavities, which are beehive-shaped in the case of CAS and cylindrical for COP. In this latter case, the surface is less robust than in the other samples with a “millefeuille” appearance.

On the other hand, the ACs differed on their surface functionalities. Table 2 compiles the analyses of the total amounts of acidic/oxygen and basic groups and PZC values. A greater presence of acidic surface groups followed the sequence COP>COM2>CAS>COM1. The opposite tendency is found for basic groups, as well as for the PCZ.

In the case of manufactured ACs, the surface chemistry is consistent with the preparation methodology; while for COP,  $H_3PO_4$  treatment caused the development of oxygen functionalities, for CAS, the high temperatures used during steam treatment (1123 K) were enough to remove most of temperature-sensitive functionalities, such as carboxylic acids [13].

**Table 2.** Point of zero Charge (PZC) and Surface functional groups ( $m_{equiv} g^{-1}$ ): Total Basic Groups (TBGs) and Total contents of acidic/polar oxygen functional groups (TOFGs)

**Tabla 2.** Punto de carga cero y grupos funcionales superficiales ( $m_{equiv} g^{-1}$ ). Grupos básicos totales y contenido total de grupos funcionales ácidos/oxígeno polar

	COM1	COM2	CAS	COP
PZC	12.2	5.8	10.6	5.5
TBGs	0.69	0.20	1.52	0.19
TOFGs	0.88	1.02	0.92	1.46

### 3.2. Nitrate adsorption

Nitrate adsorption studies were made at neutral (non-adjusted) pH and at pH 2 (with and without buffer solution added). All adsorption isotherms are collected in Figure 4 (a, b and c).

Firstly, the experiments made at neutral pH showed very unsatisfactory results in all cases, as compared with pH 2 experiments; Fig. 4.a displays adsorption isotherms with very low adsorption uptake values, especially at lower equilibrium concentrations, denoting a poor adsorption affinity in all cases. These results give evidence about the complexity of adsorption processes, where both dispersive and specific forces are involved, and where the porosity and chemistry of adsorbent and adsorbate, as well as other system features do have importance [14].

An initial explanation for the results obtained at neutral pH might be related to the adsorption media. In this way,  $OH^-$  present in solution might compete with nitrate anions for the surface adsorption sites, reducing the extent of adsorption [15].

Another important factor relates to electrostatic interactions, provided that the adsorbate has a negative charge. The ACs used in this work differ in their surface acidity, and this in turn brings out a dissimilar modification in surface charges, once they get in contact with the neutral solution. In the case of basic adsorbents (COM1 and CAS) a migration of negative charges towards the bulk on the solution is expected, and in consequence the carbon surface will be positively charged, which might favour

the participation of electrostatic attractive forces. Similarly, in acid adsorbents the movement of protons from the adsorbents surface would lead to a negatively charged surface, and thus electrostatic repulsions could be expected. The migration of charges was confirmed by measuring the solution pH in equilibrium for a given initial nitrate concentration (3  $mmol L^{-1}$ ); a pH drop was found for basic adsorbents (9.5 and 10.1, for COM1 and CAS runs, respectively), whereas a rise on it was detected for acid ones (6.1 and 5.9 for COM2 and COP, respectively).

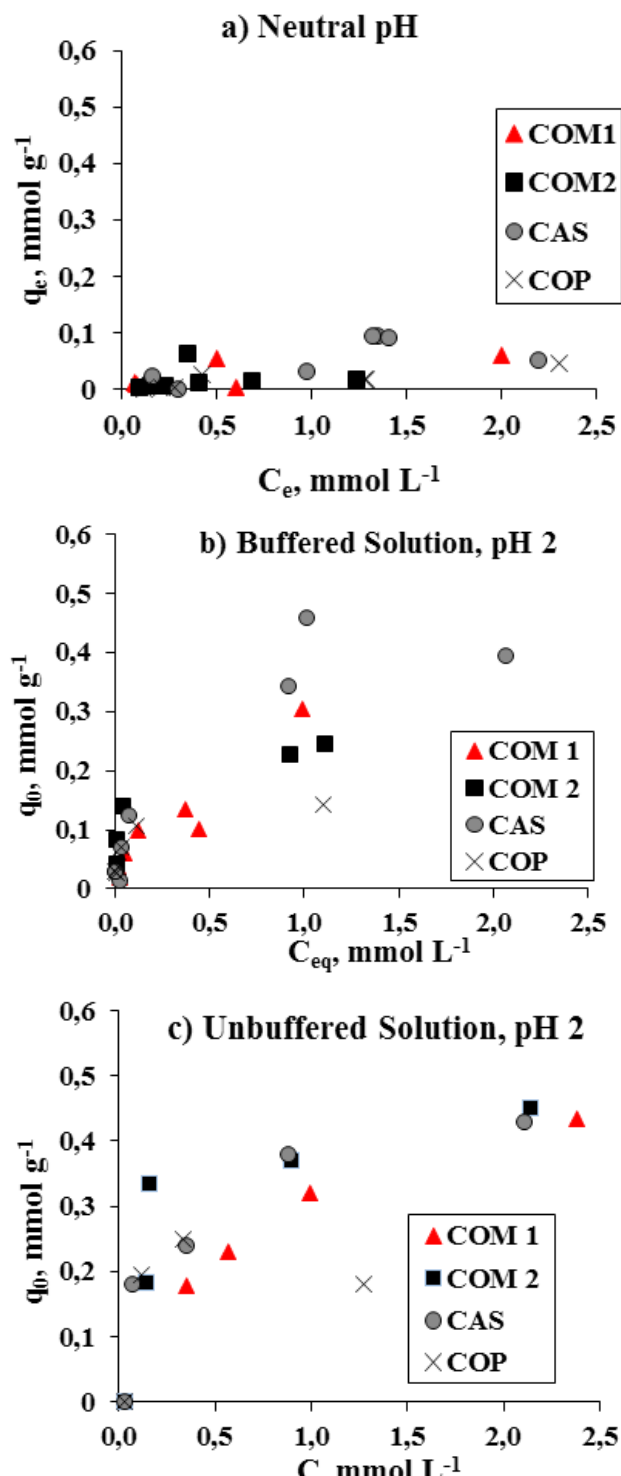


**Figure 4.** Nitrate adsorption isotherms for commercial and home-made ACs.

**Figura 4.** Isotermas de adsorción de nitrado para CAs comerciales y fabricados en el laboratorio.

On the other hand, there is another source of influence of the surface chemistry on the adsorption of nitrate

**Table 3.** Models parameters for nitrate adsorption data**Tabla 3.** Parámetros de los modelos para los datos de adsorción de nitrato

		Unbuffered solution				Buffered solution			
		COM1	COM2	CAS	COP	COM1	COM2	CAS	COP
		$q_0$ , mmol g <sup>-1</sup>							
Lang. Model	$q_0$ , mmol <sup>-1</sup>	0.449	0.410	0.438	0.305	0.418	0.256	0.896	0.191
	$R^2$	2.32	19.92	6.77	35.49	2.71	12.41	1.20	20.29
		0.989	0.998	0.999	0.999	0.884	0.989	0.805	0.925
Freund. Model	$K_f$ , (mmol <sup>-1</sup> )(Lmmol <sup>-1</sup> ) <sup>1/n</sup>	0.280	0.342	0.327	0.263	0.291	0.223	0.346	0.183
	$n$	3.06	5.77	4.88	9.30	1.67	3.69	2.01	2.85
	$R^2$	0.858	0.613	0.874	0.852	0.877	0.665	0.871	0.834

ions; in ACs, the random ordering of the aromatic sheets causes a variation in the arrangement of electron clouds in the carbon skeleton, which results in the creation of unpaired electrons and incompletely saturated valences that would undoubtedly influence the adsorption behaviour. In the particular case of nitrate ions, the availability of unpaired electrons in the adsorbent surface can be unfavourable, hindering the process. It is well established that acid surface groups are bounded at the edge of aromatic sheets and therefore tend to localize these unpaired electrons [16]. For this reason, the presence of acidic surface groups might be considered to be positive for the particular adsorption of nitrate ions.

If the participation of electrostatic interactions was relevant at neutral pH, an improvement should be expected for basic adsorbents. From our results, the influence of such contributions does not seem to have a very significant role. Also, the convenience of using acid adsorbents due to their lower availability of unpaired electrons was not verified. In summary, at neutral pH conditions nitrate adsorption is likely to be hindered, independently of the adsorbent used.

With the aim of improving such results, the reduction of the pH at a value of 2 was studied, since previous pieces of research have found that nitrate adsorption is influenced by pH, improving under acidic conditions [16]. Figures 4.b and 4.c shows the nitrate adsorption isotherms corresponding to pH 2 under unbuffered and buffered conditions. From the plots, it is seen that decreasing the pH has a positive effect on nitrate adsorption for all ACs. However, more attentive analysis reveals some differences between the results obtained with and without buffer. In order to better analyze these effects, Langmuir and Freundlich models were applied to adsorption data. Table 3 collects characteristic parameters obtained from these models. Although the fitting of the experimental data to these models was not very satisfactory in some cases (especially for Freundlich model), the analysis of the characteristic parameters can help the comparison of results. Firstly, from the adsorption isotherms for unbuffered solutions (Fig. 4.b), low nitrate uptake values are found at low equilibrium concentrations, then increasing gradually at higher values of equilibrium concentration, showing a behaviour typical of porous solids with low affinity towards the adsorbate (COM2 is an exception in this regard). Despite this effect, nitrate adsorption values up to 0.4 mmol L<sup>-1</sup> are observed. Another interesting issue is that for unbuffered solutions there are no significant differences between the adsorption values achieved in the plateau for the different ACs, nor the values of  $q_0$  as determined from Langmuir

model. Thus, the influence of both chemical and textural features might not be very relevant, as it was found at neutral pH. The improvement at pH 2 might be rather related to the lower competitiveness  $\text{NO}_3^-/\text{OH}^-$  in solution. The migration of protons to the carbon surface and thus the enhanced electrostatic attractions might be also postulated. The analysis of the pH after adsorption equilibrium showed, as in the previous case, a rapid change as a consequence of the contact AC/solution, achieving values of 7.2, 4.4, 7.6 and 3.9 for COM1, COM2, CAS and COP, respectively. On the other hand, from Figure 4.c it can be inferred that using a buffer can enhance (CAS) or decrease (COM1, COM2 and COP) the ACs' uptake capacity.

Also, if a buffered pH 2 solution is used, the surface chemistry of the adsorbents acquires a relevant role. As deduced from Figure 4.c, basic adsorbents show the best results. According to their expected higher protonation, a significant prominence of electrostatic attractive forces might be responsible for this effect. Moreover, the greater the difference between the carbon PZC and pH, the greater the density of positive charge on the adsorbent surface.

This effect was decisive, providing the best results for ASC ( $q_0=0.896 \text{ mmol g}^{-1}$ ), even despite this adsorbent had the lowest surface area. Likewise, low levels of nitrate removal attained with COP were in line with the acidic characteristics of this activated carbon. For other adsorbates, and especially for non-polar ones, the adsorption capacity is very closely related to the textural characteristics of the adsorbent [17]. Dissimilarly, in this case, the key factors governing nitrate adsorption are the solution pH and the carbon surface chemistry.

#### 4. Conclusions

Activated carbons (ACs) with different textural and surface chemistry characteristics were evaluated with the aim of getting insights about the most interesting features for improving nitrate adsorption.

Regarding home-made ACs, they were prepared from orange peel (OP) and almond shell (AS) by chemical and physical activation, respectively. These treatments conferred dissimilar features to the adsorbents: while OP carbon (COP) was very mesoporous and had a predominance of acid functionalities, AS carbon (CAS) was markedly microporous and had a basic surface. Similar trends were observed for the commercial ACs.

Nitrate adsorption studies revealed that the solution's pH had a very significant influence on the process, in such a way that it was enhanced at pH 2, which

was associated to the minimization of adsorption competition between nitrate and OH<sup>-</sup> ions. At this pH, the surface chemistry of the adsorbent was found to have a relevant role on the adsorption effectiveness; the more basic the AC, the greater the adsorption affinity towards this adsorbate, even although pore volumes were higher for acid adsorbents. This effect is remarkable and gives evidence about the need of testing any application before making a decision.

## 5. Acknowledgements

S.R. and B.L. thank the University of Extremadura for their Mobility Research Fellowship. M.E.F, G.V.N, P.R.B, and A.L.C. gratefully acknowledge Consejo Nacional de Investigaciones Científicas y Técnicas (CONICET PIP 0183), Universidad de Buenos Aires (UBA 20020100100785), and Agencia Nacional de Promoción Científica y Tecnológica (ANPCyT-FONCyT PICT 2131) from Argentina, for financial support.

## 6. References

- [1] Ferrant S, Durand P, Justes E, Probst JL, Sanchez-Perez JM. Simulating long term impact of nitrate mitigation scenarios in a pilot study basin. *Agr Water Manage* 2013; 124:85-96.
- [2] Ganesan P, Kamaraj R, Vasudevan S. Application of isotherm, kinetic and thermodynamic models for the adsorption of nitrate ions on graphene from aqueous solution. *J Taiwan Inst Chem Eng* 2013; 44:808–814.
- [3] García-Garizábal I, Causapé J, Abrahao R. Nitrate contamination and its relationship with flood irrigation management. *I J Hydrol* 2012; 442:15–22.
- [4] WHO, 2004. Drinking water quality guidelines, Recommendations, vol. 1. World Health Organization, Geneve (Switzerland), 2009. Accessed on September 2015. <[http://www.who.int/water\\_sanitation\\_health/dwq/gdwq3\\_es\\_full\\_lowres.pdf](http://www.who.int/water_sanitation_health/dwq/gdwq3_es_full_lowres.pdf)>
- [5] Ota K, Amano Y, Aikawa M, Machida M. Removal of nitrate ions from water by activated carbons (ACs)-Influence of surface chemistry of ACs and coexisting chloride and sulfate ions. *App Surf Sci* 2013; 276:838-842.
- [6] Afkhami A, Madrakian T, Karimi Z. The effect of acid treatment of carbon cloth on the adsorption of nitrite and nitrate ions. *J Hazard Mater* 2007; 144:427–431.
- [7] Nunell GV, Fernandez ME, Bonelli PR, Cukierman AL. Conversion of biomass from an invasive species into activated carbons for removal of nitrate from wastewater. *Biomass Bioenerg* 2012; 44:87-95.
- [8] De Celis J, Amadeo NE, Cukierman AL. In situ modification of activated carbons developed from a native invasive wood on removal of trace toxic metals from wastewater. *J Hazard Mater* 2009; 161(1):217–223.
- [9] González JF, Román S, Encinar J., Martínez G. Pyrolysis of various biomass residues and char utilization for the production of activated carbons. *J Anal Appl Pyrol* 2009; 85:134-141.
- [10] Sing KSW, Everett DH, Haul RAW, Moscou L, Pierotti RA, Siemieniewska T. Reporting physisorption data for gas/solid systems with special reference to the determination of surface area and porosity. *Pure Appl Chem* 1985; 57(4):613-619.
- [11] Carrott PJM, Nabais JMV, Ribeiro Carrott MML, Menendez JA. Thermal treatments of activated carbon fibres using a microwave furnace. *Micropor Mesopor Mat* 2001; 47:243–252.
- [12] Garrido J. et al., Use of N<sub>2</sub> and CO<sub>2</sub> in the Characterization of Activated Carbons. *Langmuir* 1987; 3:76-81.
- [13] Guo Y, Rockstraw DA. Activated carbons prepared from rice hull by one-step phosphoric acid activation. *Micropor Mesopor Mat* 2007; 100(1-3):12–19.
- [14] Bansal RC, Goyal M. Activated Carbon Adsorption. Ed. Taylor & Francis, New York, 2005.
- [15] Neşe ÖzTÜRK, Ennil Bektaş T. Nitrate removal from aqueous solution by adsorption onto various materials. *J Hazard Mater* 2004; 112:155-162.
- [16] Nunell GV, Fernandez ME, Bonelli PR, Cukierman AL. Conversion of biomass from an invasive species into activated carbons for removal of nitrate from wastewater. *Biomass Bioenerg* 2012; 44:87-95.
- [17] Carratalá-Abril J, Lillo-Ródenas MA, Linares-Solano A, Cazorla-Amorós D. Regeneration of activated carbons saturated with benzene or toluene using an oxygen-containing atmosphere. *Chem Eng Sci* 2010; 65:2190–2198.

# Preparation of activated carbon-metal (hydr)oxide photocatalysts under different heating conditions. Chemical aspects.

## Preparación de fotocatalizadores carbón activado-(hydr)oxídos metálicos en diferentes condiciones de calentamiento. Aspectos químicos.

A. Barroso-Bogeat, M. Alexandre-Franco, C. Fernández-González, V. Gómez-Serrano\*

Department of Organic and Inorganic Chemistry, Faculty of Sciences, University of Extremadura, 06006 Badajoz, Spain.

Departamento de Química Orgánica e Inorgánica, Facultad de Ciencias, Universidad de Extremadura, Avda. de Elvas s/n, 06006 Badajoz, España.

\*Corresponding author: vgomez@unex.es

### Abstract

This study deals with the preparation of activated carbon (AC)-metal (hydr)oxide (MO) photocatalysts from commercial AC and  $\text{Al}^{3+}$ ,  $\text{Fe}^{3+}$ ,  $\text{Zn}^{2+}$ ,  $\text{SnCl}_2$ ,  $\text{TiO}_2$  and  $\text{WO}_4^{2-}$  in water, with special emphasis on the chemical changes produced along the process. Overall, three series of samples were obtained by first soaking at 80 °C and oven-drying at 120 °C (S1) and by subsequent heating at 200 °C (S2) or 850 °C (S3) in  $\text{N}_2$  atmosphere. pH of the impregnation solution/suspension was 2.91 with  $\text{Al}^{3+}$ , 1.54 with  $\text{Fe}^{3+}$ , 5.16 with  $\text{Zn}^{2+}$ , 1.37 with  $\text{SnCl}_2$ , 5.84 with  $\text{TiO}_2$  and 9.54 with  $\text{WO}_4^{2-}$ . Data of the process yield at the three temperatures and of the ash content are reported. For S1, yield varies by  $\text{SnCl}_2 >> \text{Fe}^{3+} > \text{WO}_4^{2-} > \text{Zn}^{2+} = \text{TiO}_2 > \text{Al}^{3+}$ .

### Resumen

Se estudia la preparación de materiales de carbón activado (AC)-(hydr)oxídeos de metales (MO) a partir de un carbón activado comercial y de  $\text{Al}^{3+}$ ,  $\text{Fe}^{3+}$ ,  $\text{Zn}^{2+}$ ,  $\text{SnCl}_2$ ,  $\text{TiO}_2$  y  $\text{WO}_4^{2-}$  en disolución/suspensión acuosa, con especial énfasis en los cambios químicos producidos a lo largo del proceso. En total se han preparado tres series de muestras mediante remojo a 80 °C y secado en estufa a 120 °C (S1) y posterior calentamiento de estas muestras bien a 200 °C (S2) o a 850 °C (S3) en  $\text{N}_2$ . El pH del líquido de impregnación fue 2.91 con  $\text{Al}^{3+}$ , 1.54 con  $\text{Fe}^{3+}$ , 5.16 con  $\text{Zn}^{2+}$ , 1.37 con  $\text{SnCl}_2$ , 5.84 con  $\text{TiO}_2$  y 9.54 con  $\text{WO}_4^{2-}$ . Se aportan los datos del rendimiento del proceso y el contenido de cenizas de las muestras. Para las muestras de la serie S1, el rendimiento del proceso varía según  $\text{SnCl}_2 >> \text{Fe}^{3+} > \text{WO}_4^{2-} > \text{Zn}^{2+} = \text{TiO}_2 > \text{Al}^{3+}$ .

### 1. Introduction

The technological and economic importance of photocatalysis has increased considerably over the past decades because of the practical interest in air and water remediation, self-cleaning surfaces, self-sterilizing surfaces, and hydrogen generation using green energy of sunlight [1]. In 2009 the global market for photocatalytic products was \$848 million and with an annual growth rate of 14.3 % a global volume of \$1.7 billion was expected in 2014 [2].  $\text{TiO}_2$  is by far the most frequently employed photocatalyst, owing to the advantages of earth abundance, low toxicity, and thermal and chemical stability, besides being cheap, insoluble under most conditions, and photostable [3]. In photocatalytic reactions, metal

oxides are generally suspended in the liquid phase or dispersed over high-surface-area materials. The former process is handicapped by filtration of  $\text{TiO}_2$  fine particles and effective absorption of ultraviolet-visible radiation. In the latter process, activated carbon has been extensively researched and used as a support for  $\text{TiO}_2$  [4]. Semiconductor metal oxides are not only  $\text{TiO}_2$  but also  $\text{Al}_2\text{O}_3$ ,  $\text{Fe}_2\text{O}_3$ ,  $\text{ZnO}$ ,  $\text{SnO}_2$ , and  $\text{WO}_3$ . The preparation methods and applications for these metal oxides supported on AC were critically reviewed before [5]. Here, mainly for comparison purposes (see Ref.: 6-8), the chemical and mass changes originated as a result of the impregnation process of AC with  $\text{Al}^{3+}$ ,  $\text{Fe}^{3+}$ ,  $\text{Zn}^{2+}$ ,  $\text{SnCl}_2$ ,  $\text{TiO}_2$  and  $\text{WO}_4^{2-}$  in water and of the subsequent heat treatment of the resulting products are examined.

### 2. Experimental

Table 1. Preparation of the AC-MO catalysts. Yield and ash content.

Tabla 1. Preparación de los catalizadores AC-MO. Rendimiento y contenido de cenizas.

Series	Sample	Yield / wt%	Ash content / wt%
S1	AC	-	4.72
	A120	102	7.11
	F120	114	13.63
	Z120	103	9.73
	S120	149	27.31
	T120	103	8.82
	W120	106	9.46
S2	A200	93	8.86
	F200	94	13.55
	Z200	91	9.45
	S200	96	27.21
	T200	96	8.05
	W200	96	9.93
S3	A850	90	5.68
	F850	81	14.66
	Z850	84	6.18
	S850	68	2.34
	T850	98	9.33
	W850	95	11.54

Activated carbon (AC) from Merck (1.5 mm average particle size) and  $\text{Al}(\text{NO}_3)_3 \cdot 9\text{H}_2\text{O}$ ,  $\text{Fe}(\text{NO}_3)_3 \cdot 9\text{H}_2\text{O}$ ,  $\text{Zn}(\text{NO}_3)_2 \cdot 6\text{H}_2\text{O}$ ,  $\text{SnCl}_2 \cdot 2\text{H}_2\text{O}$  and  $\text{Na}_2\text{WO}_4 \cdot 2\text{H}_2\text{O}$  (Panreac; reagent grade), and anatase powder (Aldrich; particle size lower than 44  $\mu\text{m}$ ) in water were used in the preparation of the AC-MO. pH of the impregnation solution was in turn 2.91, 1.54, 5.16, 1.37, 5.84 and 9.54. The preparation of the samples was undertaken by wet impregnation in two successive soaking (80 °C, 5 h) and oven-drying (120 °C, 24 h) steps (S1) and subsequent heating at 200 (S2) or 850 °C (S3) for 2 h in  $\text{N}_2$  atmosphere. The yield of the process of preparation of the catalyst samples was estimated by the following expression:

$$Y(\%) = \frac{M_f(\text{g})}{M_i(\text{g})} \cdot 100 \quad (1)$$

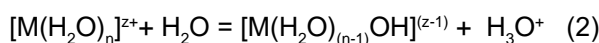
where  $M_i$  is the initial mass of AC or of the samples of series 1 and  $M_f$  is the final mass of product. The codes assigned to the catalyst samples are shown in Table 1, which also lists yield values. The ash content was determined by incineration of the samples at 650 °C for 12 h. Composition data are also compiled in Table 1.

### 3. Results and discussion

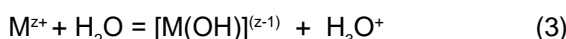
#### 3.1. Preparation of the samples

##### 3.1.1. pH of the impregnation solution

In the preparation of the AC-MO materials from AC and  $\text{Al}^{3+}$ ,  $\text{Fe}^{3+}$ ,  $\text{Zn}^{2+}$ ,  $\text{SnCl}_2$ ,  $\text{WO}_4^{2-}$  or  $\text{TiO}_2$  in water, the pH of the impregnation solution gives idea of speciation, which is an essential factor because it controls the loading process and as a last resort the mass change produced in AC. As shown in Table 1, the measured pH varies by  $\text{SnCl}_2 < \text{Fe}^{3+} < \text{Al}^{3+} <$  water  $\approx \text{Zn}^{2+} \approx \text{TiO}_2 < \text{WO}_4^{2-}$  and in the wide range between 1.37 for  $\text{SnCl}_2$  and 9.54 for  $\text{WO}_4^{2-}$ . For the  $\text{Al}^{3+}$ ,  $\text{Fe}^{3+}$  and  $\text{Zn}^{2+}$  ions, the pH variation is consistent with the tendency exhibited by these metal ions to undergo hydrolysis. Metal ions, especially in high oxidation state, in aqueous solution undergo hydrolysis by the reaction (2):



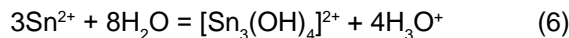
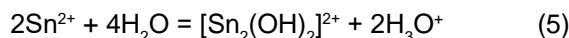
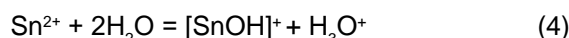
that for the sake of brevity this reaction is often written



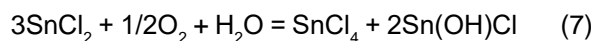
In this reaction, a proton from a water molecule in the coordination sphere of the metal ion is transferred to a water molecule in the solvent. The aquo-cation behaves as a Brönsted's acid, whereas the water molecule does as a Brönsted's base. As a result of the hydrolysis reaction, in general, metal ions in aqueous solution are found as metal aquo complexes and metal hydroxo complexes of formula  $[\text{M}(\text{H}_2\text{O})_n]^{z+}$  and  $[\text{M}(\text{H}_2\text{O})_{n-m}(\text{OH})_m]^{(z-m)+}$ , the chemical composition of these complexes being dependent on the solution concentration (i.e., 0.27 mol L<sup>-1</sup> for  $\text{Al}^{3+}$ , 0.25 mol L<sup>-1</sup> for  $\text{Fe}^{3+}$  and 0.34 mol L<sup>-1</sup> for  $\text{Zn}^{2+}$ ) and pH. The hydrolysis of  $\text{Fe}^{3+}$  begins at about pH 1 with formation of  $[\text{Fe}(\text{OH})]^{2+}$ . Likewise, , the species  $[\text{Fe}(\text{OH})_2]^+$ ,  $[\text{Fe}_2(\text{OH})_2]^{4+}$ , and  $[\text{Fe}_3(\text{OH})_4]^{5+}$  were indentified, usually at higher pH.

$\text{Al}^{3+}$  can be hydrolyzed extensively to form solutions of polynuclear hydroxides complexes and very large polymeric or colloidal species. Mononuclear species  $[\text{AlOH}]^{2+}$ - $[\text{Al}(\text{OH})_4]^-$  are also formed, the former appearing above pH 3.  $\text{Zn}^{2+}$  hydrolyzes only sparingly in acid media to produce  $[\text{ZnOH}]^+$  and  $[\text{Zn}_2\text{OH}]^{3+}$  before precipitation commences in the neutral region. In basic media,  $[\text{Zn}(\text{OH})_4]^{2-}$  and perhaps  $[\text{Zn}_2(\text{OH})_6]^{2-}$  are formed [9].

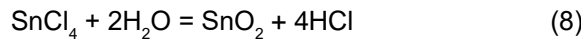
Although  $\text{SnCl}_2$  is mainly covalent in nature the electronegativities of Sn, Cl and O indicate that the Sn-Cl and Sn-O bonds possess a relatively high ionic character and therefore  $\text{SnCl}_2$  is readily soluble in water, i.e. 178 g of  $\text{SnCl}_2$  in 100 g of water at 10 °C [10]. Furthermore, it may take part in a number of equilibrium reactions depending on factors such as pH, concentration, presence of aerial oxygen, and storage time [9, 11-15]. First, in solutions at pH<2, the acidic cation  $\text{Sn}^{2+}$  easily hydrolyses by



and  $\text{Sn}^{2+}$  hydroxichlorides are formed, the trimeric species being the predominant one [9, 11, 12]. In fact, the strength of  $\text{Sn}^{2+}$  as an aqueous acid is principally as a result of the rapid polymerization of the mononuclear conjugate base [13]. At pH near 2,  $\text{SnO}\cdot\text{H}_2\text{O}$  should precipitate and transform into  $\text{SnO}$ . However, in the presence of chloride ion basic salts precipitate first [9, 12] and  $\text{SnO}$  is formed then at higher pH [14, 15]. Second, as the main hydrolytic species of  $\text{Sn}^{2+}$ ,  $[\text{SnOH}]^+$ ,  $\text{Sn}(\text{OH})_2$  and  $[\text{Sn}(\text{OH})_3]^-$  mononuclear species with diluted  $\text{Sn}^{2+}$  solutions ( $5 \times 10^{-7}$  mol L<sup>-1</sup>) and  $[\text{Sn}_2(\text{OH})_2]^{2+}$  and  $[\text{Sn}_3(\text{OH})_4]^{2+}$  polynuclear species for higher  $\text{Sn}^{2+}$  concentrations ( $10^{-3}$  and  $2 \times 10^{-2}$  mol L<sup>-1</sup>) were also reported [16 and citations therein]. Third,  $\text{SnCl}_2$  is a fair reducing agent that is slowly oxidized in aqueous solution by atmospheric oxygen [17]:



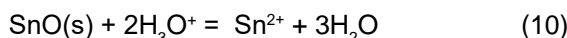
Because  $\text{SnO}_2$  is a weak base,  $\text{SnCl}_4$  in aqueous solution is hydrolyzed to considerable degree, substantially according to:



with the resulting white  $\text{SnO}_2$  remaining in solution in colloidal form. Simultaneously, HCl to some extent combines with un-reacted  $\text{SnCl}_4$  and hexachlorostannic acid,  $\text{H}_2[\text{SnCl}_6]$ , is formed [17]. Finally, during the storage of acidic  $\text{SnCl}_2$  solutions, a small precipitate was gradually formed which became visible only after 30-45 days had elapsed since their preparation. After isolation, the precipitate was made up of the phases of Sn(II,IV) hydroxychlorides and other oxo- and hydroxo-complexes [18]. Needless

to say, the low pH of the  $\text{SnCl}_2$  solution (i.e., 1.37) used in the impregnation of AC advocates for a predominance of reactions such as (4) and (8), because of a more favourable generation of HCl. In the case of the reaction (8), however, it should be taken into account that the presence of  $\text{Sn}^{4+}$  as colloidal  $\text{SnO}_2$  in such a solution should be minor due to the low concentration of  $\text{O}_2$  (i.e. presumably  $\sim 1.3 \times 10^{-3}$  mol L<sup>-1</sup> [18]) as compared to  $\text{SnCl}_2$  (i.e. 0.44 mol L<sup>-1</sup>) and also the slow kinetics of the reaction (7) [17]. As a result of the very short storage time of the  $\text{SnCl}_2$  solution (in fact, it was used immediately after preparation) before using it in the impregnation of AC, in addition to un-reacted  $\text{SnCl}_2$  and ions coming from its dissociation, it should primarily contain  $\text{Sn}^{2+}$  polynuclear species rather than  $\text{Sn}^{2+}$  and  $\text{Sn}^{4+}$  polymeric species.

After the  $\text{SnCl}_2$  solution was brought into contact with AC, i.e. the measured pH of the point of zero charge ( $\text{pH}_{\text{pzc}}$ ) for this carbon was as high as 10.50, at the onset of the soaking step, pH should increase because of the protonation of AC basic sites [19] and  $\text{SnO}$  should then be formed. The following reactions will account for the solubility of  $\text{SnO}$  in water in an acidic medium [9, 20]:



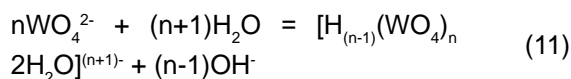
and therefore autoxidation likely went on by further embracing increased amounts of  $[\text{Sn(OH)}]^+$  and  $\text{Sn}^{2+}$ . Stannous oxide exhibits a high ability to oxidation and as a result special care was observed in its preparation to protect it from oxygen since the  $\text{Sn}^{2+}$  ion changes very rapidly to  $\text{Sn}^{4+}$  ion in the presence of atmospheric oxygen [20]. Of course, like for the  $\text{SnCl}_2$  solution, the extent to which the oxidation process occurred during the soaking step was conditioned by the small amount of  $\text{O}_2$  present in the medium. However, the opposite applies to the subsequent oven-drying step at 120 °C, which was performed in air atmosphere and therefore without no restriction to the  $\text{O}_2$  availability, apart from its low solubility. This is 3.08 cm<sup>3</sup> (gas at STP) in 100 cm<sup>3</sup>  $\text{H}_2\text{O}$  at 20 °C [21], although in the  $\text{SnCl}_2$  solution under the temperature conditions in the soaking step it should decrease not only because of the higher operating temperature (i.e. 80 °C) but also because of the presence of various inorganic chemical species in the medium. However, relating to the presence of  $\text{SnCl}_2$  in the medium, pH should not affect the  $\text{O}_2$  solubility as  $\text{Cl}^-$  is the conjugate base of the strong acid HCl. During the oven-drying step, it is likely that at the beginning the sudden water evaporation from the wetted-freshly impregnated AC prevented  $\text{O}_2$  from entering AC porosity and that, after a certain time had elapsed, the access of  $\text{O}_2$  to AC porosity was favored because of the  $\text{O}_2$  mobility and thereby diffusion ease at 120 °C.

In connection with the autoxidation of  $\text{SnCl}_2$  it was stated before that its study is complicated by the presence of a large number of ionic equilibria involving dissociation, hydrolysis and complex formation [22]. It is a thermal and photochemical chain reaction,

showing peroxide formation, induced oxidation of other molecular species present in the solution, and great sensitivity to positive and negative catalysts. The complex  $\text{HSnCl}_3$  or  $\text{H}_2\text{SnCl}_4$  was described as playing an important role in the oxidation of  $\text{SnCl}_2$  [23]. Furthermore, one such positive catalyst is activated carbon, which accelerated the reaction but not in proportion to the weight used [24]. Air-induced oxidation of organic and inorganic systems goes through free radical processes. Autoxidation reactions are usually subdivided into initiation, propagation and termination reactions. Two types of initial reactions can take place: abstraction of H atoms from various bonds and addition of  $\text{O}_2$  to the free radical sites [25]. Molecular oxygen adds and gives peroxy radicals, yet  $\text{O}_2$  can also act directly as an oxidant (i.e., electron acceptor) [26]. Since chemical species such as peroxides are stronger oxidants than molecular  $\text{O}_2$  (i.e., as a guide,  $E^\circ$  is 1.776 V for  $\text{H}_2\text{O}_2$  and 1.229 V for  $\text{O}_2$  [10]), it can be presumed that in the autoxidation of  $\text{SnCl}_2$  AC behaved simultaneously as a catalyst of the reaction and as a reactant that could also be oxidized.

Titanium dioxide (anatase) shows a high tendency to hydroxylation [27]. For hydrated titania obtained by hydrolysis of titanium salts it was assumed that its surface is completely hydroxylated. However drying, even at room temperature, leads to irreversible dehydroxylation [28]. Water adsorption on strongly dehydroxylated anatase takes place in two ways: part of the water molecules are dissociated forming hydroxyl groups again, while the major part of water is adsorbed molecularly [29]. Repetition of the hydroxylation and dehydroxylation cycles leads to a decreasing concentration of the sites for dissociative adsorption, probably owing to surface reconstructions [30]. Accordingly, it seems that after the contact with water already hydroxylated anatase only underwent a slight hydroxylation, in accord with the small pH change produced for the  $\text{TiO}_2$  suspension in respect to deionized water.

According to the Pourbaix's diagram for tungsten, the only ionic species stable in aqueous solution at basic pH is the tungstate ion,  $\text{WO}_4^{2-}$ , whereas the existence of pertungstic ion  $\text{WO}_5^{2-}$  remains hypothetical [31]. Because of hydration, structures such as  $[\text{WO}_2(\text{OH})]^{1-}$  and  $[\text{W}(\text{OH})_8]^{2-}$  were proposed as well for the  $\text{WO}_4^{2-}$  ion in aqueous solution at pH ≥ 6 [32]. The pH of 9.54 measured for the  $\text{Na}_2\text{WO}_4 \cdot 2\text{H}_2\text{O}$  solution falls within the range of pH values between 9.15 and 10.5 reported in the literature for molar solutions prepared from  $\text{Na}_2\text{WO}_4 \cdot 2\text{H}_2\text{O}$  and purified water [33]. The alkalinity of the  $\text{WO}_4^{2-}$  solution may be due to the presence of excess alkali (i.e., NaOH) in commercial  $\text{Na}_2\text{WO}_4 \cdot 2\text{H}_2\text{O}$  or to  $\text{Na}_2\text{WO}_4$  hydrolysis and polymerization in accord with the postulated basic mechanism in the formation of iso- and heteropolytungstates from  $\text{WO}_4^{2-}$  [33]:



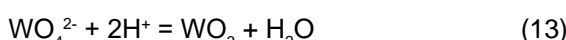
### 3.1.2. Yield

The yield of the impregnation process of AC for S1 data in Table 1 is higher than 100% for all samples and strongly dependent on the MO precursor. Thus,

it varies in the wide range between 102 wt% for A120 to 149 wt% for S120 by S120 > F120 > W120 > Z120 = T120 > A120 and is markedly higher for F120 and very especially for S120 than for the rest of the samples belonging to S1. Probably, two important factors with influence on the process yield are the diffusion of the MO precursor in pores of AC and the metal density. Diffusion will be mainly dependent on the size of the MO precursor, which may be found as a hydrated, hydrolyzed or polymerized metal ion and also as a hydroxylated MO in the aqueous system. In the case of S120, mass balance is consistent with the involvement of small size tin species (e.g.,  $\text{Sn}^{2+}$  and  $[\text{Sn}(\text{OH})]^+$ ), generated from  $\text{SnCl}_2$ , in the diffusion process and with their subsequent oxidation catalyzed by AC, which should ultimately give tin species with a high oxygen content such as  $\text{SnO}_2$ . For  $\text{Fe}^{3+}$ , polynuclear hydrolyzed species may be formed in the 0.25 mol L<sup>-1</sup> solution by the reaction [34]:



Likewise,  $\text{WO}_4^{2-}$  should transform into  $\text{WO}_3$  by:



despite the high pH of the  $\text{WO}_4^{2-}$  solution and AC's surface (i.e., pH of the point of zero charge is 10.5 for AC). Probably, the reaction (13) was favoured by the evaporation of water during the oven-drying step. Finally, from the low yield for T120 it is evident the influence of particle size on the impregnation process of AC. On the other hand, the latter is also an important factor in connection with the process yield because of the wide set of metal precursors used in the study. Density is a function of the metal atomic mass, which determines the weight of a given amount of sample and for the here used MO precursors it ranges between 26.981 for Al and 183.85 for W [33]. On the other hand, yield varies between 91-96 wt% for S2 and 68 - 98 wt% for S3, and therefore in a wider range for S3 than for S2.

### 3.1.3. Ash content

As can be seen in Table 1, for a large number of AC-MO samples, the ash content is about twice higher than for AC. For S850, however, it is noticeably lower than for AC. For S1, the ash content varies by S120 > F120 > Z120 > W120 > T120 > A120, the correlation with yield being as a rule good. The slightly different ash contents for homologous samples of S1 and S2 argue for a reversible desorption of water and partial dehydroxylation of S1 in the preparation of S2, because of the 200 °C-low heat treatment temperature. On the contrary, for S3 the ash content varies by F850 > W850 > T850 > Z850 > A850 > S850 and widely between 2.34 wt% for S850 and 14.66 wt% for F850. The ash content is low not only for S850 but also for A850 and Z850, whereas it is high for F850 and W850. Accordingly, it is attributable to the carbothermal reduction of  $\text{M}_n\text{O}_m$ :



that originates CO release and M. Lower-melting

point metals (i.e. Sn, 231.93 °C; Zn, 419.53 °C; Al, 660.32 °C) will melt and vaporize, whereas higher-melting point metals (i.e. Fe, 1538 °C; W, 3414 °C) will remain unaltered in the samples. This influenced the ash content as both metals should be oxidized again to  $\text{M}_n\text{O}_m$  during the incineration process of the samples.

### Conclusions

The preparation of AC-MO photocatalysts from AC and  $\text{Al}^{3+}$ ,  $\text{Fe}^{3+}$ ,  $\text{Zn}^{2+}$ ,  $\text{SnCl}_2$ ,  $\text{TiO}_2$  or  $\text{WO}_4^{2-}$  in water has been thoroughly studied by taking into account the concentration and pH, and thereby speciation, of the impregnation solution. For S1, the process yield varies by S120 > F120 > W120 > Z120 = T120 > A120 and ranges between 102 wt% for A120 and 149 wt% for S120. The mass changes as a rule are stronger for S1 and S3 than for S2. The ash content is higher for F120 and especially for S120 than for the remaining samples. A number of metal oxides are carbothermally reduced at 850 °C and the resulting metal may melt and vaporize, depending on melting temperature relative to heat treatment temperature. The ash content becomes as low as 2.34 wt% for S850.

### Acknowledgements

Financial support by Junta de Extremadura and European FEDER Funds is gratefully acknowledged. A. Barroso-Bogeat thanks Spanish Ministry of Education, Culture and Sport for the concession of a FPU grant (AP2010-2574).

### References

- [1] Li WX. Photocatalysis of oxide semiconductors. *J. Aust. Ceram. Soc.* 2013; 49: 41-46.
- [2] Gagliardi MM. Photocatalysts: Technologies and global marked. BBC Research Report (AVM069A); March 2010.
- [3] Mills A, Davies RH, Worsley D. Water purification by semiconductor photocatalysis. *Chem. Soc. Rev.* 1993; 22: 417-425.
- [4] Gianluca LP, Bono A, Krishnaiah D, Colling JD. Preparation of titanium photocatalyst loaded onto activated carbon support using chemical vapor deposition: A review paper. *J. Hazard. Matter.* 2008; 157: 209-219.
- [5] Barroso-Bogeat A, Fernández-González C, Alexandre-Franco M, Gómez-Serrano V. Activated carbon as a metal oxide support: A review. In: James F. Kwiatkowski editor. *Activated carbon: Classifications, Properties and Applications*. Nova Science Publishers, Inc. 2012, p. 297-318.
- [6] Barroso-Bogeat A, Alexandre-Franco M, Fernández-González C, Gómez-Serrano V. Activated carbon surface chemistry: Changes upon impregnation with Al(III), Fe(III) and Zn(II)-metal oxide catalyst precursors from  $\text{NO}_3^-$  aqueous solutions. *Arab. J. Chem.*, <http://dx.doi.org/10.1016/j.arabjc.2016.02.018>.
- [7] Barroso-Bogeat A, Alexandre-Franco M, Fernández-González C, Gómez-Serrano V. Preparation of activated carbon- $\text{SnO}_2$ ,  $\text{TiO}_2$ , and  $\text{WO}_3$  catalysts. Study by FT-IR spectroscopy. *Ind. Eng. Chem. Res.* 2016; 55: 5200-5206.
- [8] Barroso-Bogeat A, Alexandre-Franco M, Fernández-González C, Gómez-Serrano V. Preparation of activated carbon-metal (hydr)oxide materials by thermal methods. Thermogravimetric-mass spectrometric (TG-MS) analysis. *J. Anal. Appl. Pyrol.* 2015; 116: 243-252.
- [9] Baes CF Jr., Mesmer RE. *The Hydrolysis of Cations*. John Wiley & Sons, New York, 1976.
- [10] In: D.R. Lide (Ed.), *CRC Handbook of Chemistry and Physics*, 2005-2006 86<sup>th</sup>ed., Taylor & Francis, Boca Raton,

2005.

[<sup>11</sup>] Tobias RS. Studies on the hydrolysis of metal ions. 21. The hydrolysis of tin (II) ion,  $\text{Sn}^{2+}$ . *Acta Chem. Scand.* 1958; 12: 198-223.

[<sup>12</sup>] Ortiz A, Mendoza M, Rodríguez Paez JE. Naturaleza y formación de complejos intermedios del sistema  $\text{SnCl}_2 \cdot \text{NH}_4\text{OH} \cdot \text{H}_2\text{O}$ . *Mater. Res.* 2001; 4: 265-272.

[<sup>13</sup>] Tobias RT, Hugus ZZ. Least squares computer calculations of chloride complexing on tin(II), the hydrolysis of tin(II), and the validity of the ionic medium method. *J. Phys. Chem.* 1961; 65: 2165-2169.

[<sup>14</sup>] Burriel F, Conde F, Arribas S, Hernández J. *Química Analítica Cualitativa*, Paraninfo, Madrid, 1994.

[<sup>15</sup>] Ararat C, Varela JA, Rodríguez-Páez JE. Uso de métodos químicos para obtener polvos cerámicos del sistema  $(\text{Sn}, \text{Ti})\text{O}_2$ . *Bol. Soc. Esp. Ceram.* V. 2005; 44: 215-222.

[<sup>16</sup>] Séby F, Potin-Gautier M, Giffaut E, Donard OFX. A critical review of thermodynamic data for inorganic tin species. *Geochim. Cosmochim. Acta* 2001; 65: 3041-3053.

[<sup>17</sup>] Remi H. *Treatise on Inorganic Chemistry*, Vol. 1, Elsevier, Amsterdam, 1956.

[<sup>18</sup>] Reva OV, Vorob'eva TN. Oxidation, hydrolysis and colloid formation in storage of  $\text{SnCl}_2$  aqueous solutions. *Russ. J. Appl. Chem.* 2002; 75: 700-705.

[<sup>19</sup>] Leon y Leon CA, Solar JM, V. Calemma, Radovic LR. Evidence for the protonation of basal plane sites on carbon. *Carbon* 1992; 30: 797-811.

[<sup>20</sup>] Garrett AB, Heiks RE. Equilibria in the stannous oxide-sodium hydroxide and in the stannous oxide-hydrochloric acid systems at 25 °C. Analysis of dilute solutions of stannous tin. *J. Am. Chem. Soc.* 1941; 63: 562-567.

[<sup>21</sup>] N.N. Greenwood, A. Earnshaw, *Chemistry of the Elements*, Pergamon Press, Oxford, 1989.

[<sup>22</sup>] Lachman SJ, Tompkins FC. The autoxidation of inorganic reducing agents. Part II. Stannous chloride (experimental). *Trans. Faraday Soc.* 1944; 40: 130-136.

[<sup>23</sup>] Haring RC, Walton JH. The autoxidation of stannous chloride. IV The effect of some non-aqueous solvents. *J. Phys. Chem.* 1934; 38: 153-160.

[<sup>24</sup>] Haring RC, Walton JH. The autoxidation of stannous chloride. II A survey of certain factors affecting this reaction. *J. Phys. Chem.* 1933; 37: 133-145.

[<sup>25</sup>] Simic MG. Free radical mechanism in autoxidation processes. *J. Chem. Educ.* 1981; 58: 125-131.

[<sup>26</sup>] Simic M, Hayon E. Comparison between the electron transfer reactions from free radicals and their corresponding peroxy radicals to quinines. *Biochem. Biophys. Res. Commun.* 1973; 50, 364-369.

[<sup>27</sup>] Huang WF, Chen HT, Lin MC. The adsorption and reactions of  $\text{SiCl}_c$  ( $c = 0-4$ ) on hydroxylated  $\text{TiO}_2$  anatase (101) surface: A computational study on the functionalization of titania with  $\text{Cl}_2\text{Si}(\text{O})\text{O}$  adsorbate. *Comput. Theor. Chem.* 2012; 993: 45-52.

[<sup>28</sup>] Hadjiivanov KI, Klissurski DG. Surface chemistry of titania (anatase) and titania-supported catalysts. *Chem. Soc. Rev.* 1996; 25: 61-69.

[<sup>29</sup>] Morterra C. An infrared spectroscopic study of anatase properties. *J. Chem. Soc., Faraday Trans. 1* 1998; 84: 1617-1637.

[<sup>30</sup>] Primet M, Pichat P, Mathieu M-V. Infrared study of the surface of titanium dioxides. *J. Phys. Chem.* 1971; 75: 1216-1221.

[<sup>31</sup>] Barré T, Arurault L, Sauvage FX. Chemical behavior of tungstate solutions. Part 1. A spectroscopic survey of species involved. *Spectrochim. Acta, Part A* 2005; 61: 551-557.

[<sup>32</sup>] Lassner E, Schubert WD. *Tungsten: Properties, Chemistry, Technology of the Element, Alloys and Chemical Compounds*, Kluwer Academic, New York, 1999.

[<sup>33</sup>] Freedman MJ. Polymerization of anions: The hydrolysis of sodium tungstate and sodium chromate. *J. Am. Chem. Soc.* 1958; 80: 2072-2077.

[<sup>34</sup>] Milburn, RM, Vosburgh, WC. A spectrophotometric study of the hydrolysis of iron(III) ion. II. Polynuclear species. *J. Am. Chem. Soc.* 1955; 75: 1352- 1355.

# Electrochemically modified carbon materials for applications in electrocatalysis and biosensors

C. González-Gaitán

Presented in 2016, Instituto Universitario de Materiales. Universidad de Alicante.

Supervisors: R. Ruiz-Rosas and D. Cazorla-Amorós (Universidad de Alicante).

## OBJECTIVES AND NOVELTY

The present work focused in the functionalization of nanostructured carbon materials for their application as electrocatalysts for the oxygen reduction reaction at the cathode of fuel cells and as transducer elements in electrochemical biosensors.

### Fuel Cells

Nowadays, there is an increase in the use and consumption of energy in the world and until now the fossil fuels cover this demand. There is the necessity of the use of renewable energies; however, since they are discontinuous, devices for energy storage and production are needed. In this sense, several devices have been developed during the last decades, in which the fuel cells appears as a good alternative to replace/combine the combustion engines. Fuel cells can be applied in various industries such as automotive, stationary and portable energy generation and supply for emergency systems. These devices have several advantages compared to conventional technologies that are used for energy production: (i) can operate with higher efficiency than the combustion engines; (ii) can convert chemical energy from a fuel into electric energy with efficiency close to 60%; (iii) have lower emissions than the conventional combustion engines. However, there are several aspects that still are in development for their use in practical applications.

The reaction that occurs in the cathode is the Oxygen Reduction Reaction (ORR). The ORR is a reaction with a slow kinetics, which makes necessary the use of a catalyst. The challenge is to develop new electrocatalysts with high performance and durability at lower prices. Even though platinum is the best catalyst, when supported on carbon materials, such materials are expensive and vulnerable to poisoning and electrochemical deactivation, which affect their efficiency and useful life. For that reason, it is necessary to explore new electrocatalytic materials of lower costs. Therefore the focus is on catalysts with non-noble metals or metal-free, which are less expensive, robust to the deactivation or poisoning and highly available in nature.

### Biosensors

Glucose detection has been studied for many years because of its implication in diseases as diabetes and hypoglycemia. They are caused by metabolic disorders in which the body does not produce the necessary amount of insulin for glucose processing, leading to glucose levels out of the normal concentration range (4.0 to 5.9 mM). The diagnosis and supervision of these diseases leads to a high demand for blood glucose monitoring systems and huge efforts have been done in the development of novel sensors.

The development of biosensors based on glucose

oxidase enzyme (GOx) is seen as the most promising technology to achieve accurate, non-invasive and even continuous monitoring of sugar levels, and research on this field has witnessed a remarkable activity. The use of this specific enzyme leads to an increase in the selectivity and the sensitivity of the sensor, minimizing the possible interferences with other analytes present in biological fluids. The limiting factor in the glucose biosensors is the electron transfer between the FAD and the electrode surface. The use of nanostructured carbon materials has been studied as electrode materials in order to enhance the electronic transfer, which results in an increase of the selective recognition, and in an enhancement of the detection limit.

## RESULTS

### *Electrochemical functionalization of carbon nanotubes (CNTs) and Zeolite Tempered Carbon (ZTC) with aminobenzene acids*

The functionalization of CNTs with aminobenzene acids has been performed using potentiodynamic methods at oxidative conditions. The functionalization was confirmed by XPS and electrochemical measurements. An increase in the nitrogen, sulfur and phosphorus content was seen for the 4-aminobenzoic (4-ABA), 4-aminobenzene sulfonic (4-ABSA) and 4-aminobenzyl phosphonic (4-ABPA) acids functionalized CNTs, respectively. A noticeable increase in the capacitance for the functionalized CNTs points out the formation of an electroactive polymer thin film on the CNTs surface along with covalently bonded functionalities (Fig. 1a).

The ORR activity was studied in basic medium using a RRDE. The ORR activity of the functionalized samples was similar to that of the parent CNTs, independently of the functional group present in the aminobenzene acid. A heat treatment in a slightly oxidizing atmosphere at 800 °C of the CNTs functionalized with aminobenzoic acid produced a material with high amounts of surface oxygen and nitrogen groups, that seem to modulate the electron-donor properties of the resulting material, which enhance the ORR activity (NT-ABA\_800\_O in Fig. 1b). These are promising results that validates the use of electrochemistry for the synthesis of novel N-doped electrocatalysts for ORR in combination with adequate heat treatments.

A selective electrochemical functionalization of a zeolite templated carbon (ZTC) with two different aminobenzene acids (2-ABA and 4-ABA) was performed. The optimization of the functionalization conditions was achieved in order to preserve the unique ZTC structure. It was possible to avoid the electrochemical oxidation of the highly reactive ZTC structure by controlling the potential limit of the potentiodynamic experiment. The electrochemical characterization demonstrated the formation of

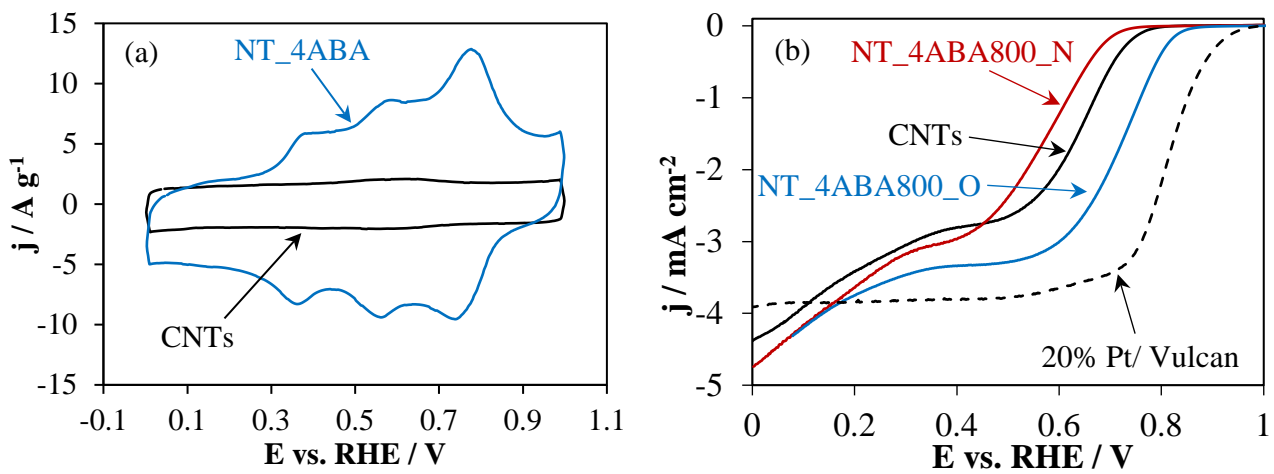


**Fig. 1** (a) CV of CNTs and functionalized nanotubes with 4-ABA (NT\_4ABA). (b) LSV of NT-4-ABA based samples at 1600 rpm, 5 mV s<sup>-1</sup>

polymer chains along with covalently bonded functionalities to the ZTC surface (Fig. 2). The success of the proposed approach was also validated by using TPD, XPS and FTIR, which confirmed the presence of different nitrogen groups in the ZTC surface. This method could be used to achieve highly selective functionalization that could enhance the electro-oxidation resistance and increase the capacitance of highly porous carbon materials.

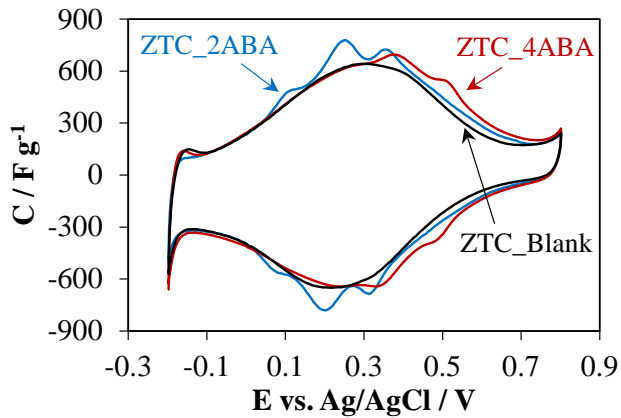


**Fig. 2** CV of functionalized ZTC with 2-ABA and 4-ABA.

#### Iron (FePc) and Cobalt (CoPc) phthalocyanines supported con CNTs as electrocatalysts for the ORR

Catalysts based in FePc and CoPc loaded CNTs were prepared. The catalysts were heat treated at different temperatures and atmospheres in order to change the surface chemistry of the pristine CNTs. The role of those functionalities in the activity and stability as electrocatalysts for the ORR in alkaline medium was studied. The prepared catalysts displayed an enhanced activity towards ORR compared to the pristine CNTs.

The samples based in FePc showed a better performance than the CoPc-based samples, with equivalent performance to the state-of-the-art Pt-C catalyst even with very low amount of metal (Table 1). According to the temperature of the heat treatment, changes in the chemical properties of the materials are produced, which showed an enhanced activity when the samples are heat treated at 400 °C where a stronger interaction of the FePc with the CNTs is

observed. Additionally, the use of functionalized carbon nanotubes with oxidized nitrogen species as support showed that the presence of such functionalities leads to a decrease in the ORR activity, since they prevent the π-π interaction between the CNTs surface and the FePc. Finally, stability tests were performed and it was found that the fast deactivation seems to be related to the H<sub>2</sub>O<sub>2</sub> formation during the experiments.

**Table 1.** Electrochemical parameters calculated from the RRDE experiments of the electrocatalysts

Sample	E <sub>onset</sub> vs. RHE / V	% H <sub>2</sub> O <sub>2</sub> at 0.4 V
NTs	0.74	89
NT_CoPc	0.83	48
NT_CoPc_400	0.83	59
NT_CoPc_800	0.85	83
NT_FePc	0.92	10
NT_FePc_400	0.94	7
NT_FePc_800	0.88	59
20% Pt-C	0.97	4

#### Glucose biosensors based on CNTs

The development of glucose electrochemical sensors have been carried out by the immobilization of GOx on CNTs with different structures: tubular and herringbone CNTs. The CNTs were previously modified using chemical and electrochemical methods in order to change the surface chemistry and study the influence in the enzyme immobilization.

The results show that all GOx-loaded materials were active to the glucose detection using different approaches: (i) the detection of the H<sub>2</sub>O<sub>2</sub> formed

during the reaction at 0.45 V, (ii) the introduction of a mediator as an electron carrier between the glucose and the FAD at 0.2 V and (iii) the detection at negative potentials, i.e. at -0.4 V, which is close to the potential of the FAD/FADH<sub>2</sub> redox processes. The best results were achieved with oxidized samples, which are proposed to immobilize a larger amount of active enzymes owing to the presence of carboxylic functionalities.

The use of negative potentials leads to remove the interference problems with other analytes usually present in the biological fluids. Glucose detection in an O<sub>2</sub> saturated atmosphere at -0.4 V for oxidized herringbone CNTs, this glucose biosensor shows a linear detection range between 0.03 and 4 mM with a sensitivity of 1.07 μA mM<sup>-1</sup> and a detection limit of 0.01 mM. The biosensor based in oxidized tubular CNTs shows a linear detection range between 0.3 and 7 mM, and a sensitivity of 0.804 μA mM<sup>-1</sup> with a detection limit of 0.1 mM.

## CONCLUSIONS

The main contribution of this work was the functionalization of nanostructured carbon materials using conventional chemical and thermal treatment methods and novel electrochemical methods. The electrochemical functionalization with different aminobenzene acids was successfully performed using carbon nanotubes and ZTC. The conditions were optimized in order to preserve the structure of the materials, changing the surface chemistry of the pristine materials.

The prepared materials were tested in two different applications; as electrocatalysts for the ORR and as transducer elements of biosensors for glucose detection. The functionalized materials showed an enhanced ORR activity depending on the functionalization and heat treatment performed to the materials. The metal-free catalysts showed a good performance when an oxidant atmosphere was used during the heat treatment, due to the combination of oxygen and nitrogen functionalities that modulate the electron-donor properties in the activity. FePc based catalyst showed an excellent ORR catalyst performance – close to the Pt-based catalyst – with a small amount of metal loading.

Likewise, biosensors for glucose detection were prepared by adsorption of GOx on the modified carbon materials. The glucose detection was performed by using different approaches: the detection of the H<sub>2</sub>O<sub>2</sub> formed during the reaction at 0.45 V, the introduction of a mediator as an electron carrier between the glucose and the FAD at 0.2 V and the detection at -0.4 V.

## RELATED PUBLICATIONS

[1] González-Gaitán C, Ruiz Rosas R, Nishihara H, Kyotani T, Morallón E, Cazorla-Amorós D. Successful functionalization of superporous zeolite templated carbon using aminobenzene acids and electrochemical methods, *Carbon*, 2016; 99, 157 - 166.

[2] González-Gaitán C, Ruiz Rosas R, Morallón E, Cazorla-Amorós D. Electrochemical methods to functionalize carbon materials. In *Chemical functionalization of Carbon Nanomaterials: Chemistry and Applications*, Taylor & Francis Group, 2015; 231 - 249.28/07/2015.

[3] González-Gaitán C, Ruiz Rosas R, Morallón E, Cazorla-Amorós D. Functionalization of carbon nanotubes using aminobenzene acids and electrochemical methods. Electroactivity for the oxygen reduction reaction, *International Journal of Hydrogen Energy*, 2015; 40, 11242 - 11253.

*Full Thesis can be downloaded from [www.ua.es](http://www.ua.es)*

# Doped carbon material electrodes for energy applications

A.C. Ramírez-Pérez

Presented in 2016, Instituto Universitario de Materiales, Facultad de Ciencias. Universidad de Alicante, 03080, Alicante, Spain.

SUPERVISORS: Diego Cazorla Amorós and Emilia Morallón Núñez.

\*Corresponding autor: [anacristina.ramirez@ua.es](mailto:anacristina.ramirez@ua.es)

## OBJECTIVES AND NOVELTY

Carbon materials have many advantages such as lightweight, chemical stability, electrical conductivity and both porosity and surface chemistry that can be tailored. These materials play an important role in devices for generation and storage of energy, like fuel cells and supercapacitors. However, in these fields the performance of the carbon materials depends on the porosity and the surface chemistry. In order to improve their properties, the use of N-doped carbon materials has been proposed; these N-doped carbon materials can be obtained by different methods. In this work, we have selected a nitrogen-rich polymer (polypyrrole, PPy) as precursor of N-doped carbon materials. PPy-based materials were obtained by adsorption from different concentrations of Py monomer on commercial activated carbon fibers (ACF). After the chemical polymerization was performed, the N-doped activated carbon samples were prepared by carbonization at different temperatures.

Additionally, the use of electrochemically active metal oxides can improve the capacitance of porous carbon materials by the incorporation of pseudocapacitance. Then, the mixture of a superporous activated carbon (AC) obtained from Spanish anthracite and metal oxides ( $\text{Co}_3\text{O}_4$  and  $\text{CuCo}_2\text{O}_4$ ) at different percentages have been prepared. Six different composite materials were prepared in order to evaluate their electrochemical performance and the influence of the metal oxides in the electrochemical properties of the AC.

All the samples (N-doped carbon materials and composites AC/metal oxides materials were characterized using different techniques: XPS, SEM, elemental analysis, XRD, physical adsorption of  $\text{N}_2$ , cyclic voltammetry. The most relevant were selected to be used as electrodes in supercapacitors and as catalysts in the oxygen reduction reaction (ORR).

## RESULTS

### PPy-based materials

Table 1 shows (as an example) the textural properties of selected carbon materials. Then, it can be observed an important decrease in the adsorption

capacity after polymerization of PPy into the porosity of the activated carbon fibers (F). This decrease could be due to the presence of the PPy film over the surface of the fibers, as observed with PANI[1]. After carbonization, the small increase in the adsorption capacity observed is a consequence of the PPy carbonization.

The analysis of XPS N 1s spectra for FP5 indicates the presence of 2 peaks in the sample. The main signal appear at 400.1eV which is characteristic of pyrrolic-nitrogen[2][3]. The second signal at lower binding energy can be assigned to the iminic nitrogen (BE=398.6eV)[2]. After carbonization, important changes occur in the XPS. The heat treatment at 500 °C results in two XPS peaks that appear at different binding energies. One of them is associated to pyridine groups (398eV) and the second one with positively charged N functionalities such as pyrrole and/or pyridone groups (400.7eV)[3][4]. After heat treatment at 800 °C the second peak shifts to higher binding energies and can be attributed to quaternary N (400.7eV). These functionalities appear due to the condensation reactions that take place at these temperatures

The electrochemical properties of the samples were investigated by cyclic voltammetry (CV) at a relatively slow scan rate ( $5\text{mV}\cdot\text{s}^{-1}$ ) and galvanostatic charge-discharge cycles at different current densities. The results indicate that the main contribution to capacitance is the charge and discharge of the double layer.

Durability tests were made by the evolution of the capacitance during 2000 charge-discharge cycles in two electrodes cell configuration (Table 1) at 1.4 V and at 0.5 A/g. The results show that the heat treated samples present the highest initial capacitance and capacitance retention in comparison to the original material. This result is attributed to the presence of positively charged nitrogen species and pyridinic groups on the carbon material surface. Moreover, these N-functional groups increase the wettability of the electrode which facilitates interactions with the electrolyte. Nonetheless the presence of the polypyrrole does not imply a better performance of the carbon materials.

**Table 1.** Porous texture characterization. Quantification of Nitrogen containing. Values of capacitance and its retention after 2000cycles of charge-discharge at 0.5 A/g in 1M  $\text{H}_2\text{SO}_4$ . Onset potential obtained in RRDE configuration for ORR

Sample	$A_{BET}$ [m <sup>2</sup> /g]	$V_{DR}(\text{N}_2)$ [cm <sup>3</sup> /g]	$V_{DR}(\text{CO}_2)$ [cm <sup>3</sup> /g]	N%	$C_0$ [F/g]	$C_f$ [F/g]	$C/C_0$ [%]
F	1919	0.8	0.4	--	47	46	97
FP5	1125	0.5	0.3	2.2	30	4	13
FP55	1366	0.6	0.6	2.1	54	52	96
FP58	1435	0.6	0.6	1.4	50	48	96

### AC-Metal oxides materials

Two kinds of spinel nanoparticles were synthesized,  $\text{Co}_3\text{O}_4$  and  $\text{CuCo}_2\text{O}_4$ ; both of them were characterized by different physicochemical techniques. The characterization by cyclic voltammetry is in agreement with the structural data obtained by XRD and XPS. The typical cyclic voltammetry of this kind of oxides is obtained; it contains two peaks corresponding to the two redox processes of these spinel electrodes. An activated carbon was prepared by activation with KOH of Spanish anthracite, showing high micropore volume and a narrow micropore size distribution. The combination of these two kinds of materials (activated carbon and metal oxides nanoparticles) was used to prepare composite materials by physical mixing. These composite materials have been used as electrodes in supercapacitors in alkaline conditions and in the reaction of oxygen reduction.

All the samples where used as catalysts in ORR being the carbon materials obtained up to 800°C the ones that have the higher catalytic activity due to the higher concentration in pyridine and quaternary N functionalities[5][6].

The catalytic activity of the AC stands out with respect to the rest of the materials studied in this Thesis. This seems to be related with the higher porosity development in this material which can increase the residence time of the oxygen molecules and the peroxide species improving the electrochemical activity towards the complete reduction of the oxygen molecule. The addition of cobalt based metal oxides in the superporous activated carbon does not imply an increase in the electrochemical activity, which seems to be due to the decrease in porosity of the composite material. However, an increase in the selectivity of the reaction towards the complete reduction of oxygen molecule is observed.

### CONCLUSIONS

The results obtained in this Ph.D. Thesis support that carbon materials are among the most suitable for supercapacitor and catalysis applications due to their physicochemical properties, such as high surface area and possibility of tailoring both the surface chemistry and porosity. These characteristics can be selected in order to improve both the performance of carbon-based supercapacitors and their catalytic properties. The use of conducting polymers and metal oxides provides an interesting alternative for improving the properties of the typical activated carbon materials. Thus, two kinds of carbon materials based on polypyrrole were synthesized by heat treatment in inert atmosphere at two different temperatures, showing the presence of nitrogen surface groups. At high temperatures, quaternary and pyridinic groups predominate. Composite materials based on PPy and activated carbon fibers containing nitrogen species between 1 and 4wt% are prepared. The capacitors built with the N-doped activated carbon fibers materials after carbonization, have a better performance in terms of capacitance and durability than the pristine activated carbon fibers. This confirms the beneficial contribution of nitrogen functional groups. The capacitors show a high durability at a voltage of 1.4V in comparison to the capacitor prepared with the activated carbon fibers. The supercapacitors based on the metal

oxide/activated carbon materials show that small quantities of oxides nanoparticles ( $\text{Co}_5\text{A}95$  and  $\text{CuCo}_5\text{A}95$ ) increase the capacitance and stability of the capacitor. The addition of cobalt based metal oxides in the superporous activated carbon does not imply an increase in the activity in the ORR, which seems to be due to the decrease in porosity of the composite material. However, an increase in the selectivity of the reaction towards the complete reduction of oxygen molecule is observed.

### RELATED PUBLICATIONS

- [1] D. Salinas-Torres, J. M. Sieben, D. Lozano-Castelló, E. Morallón, M. Burghammer, C. Riekel, and D. Cazorla-Amorós, "Characterization of activated carbon fiber/polyaniline materials by position-resolved microbeam small-angle X-ray scattering," *Carbon*, vol. 50, pp. 1051–1056, 2012.
- [2] A. Morozan, P. Jégou, S. Campidelli, S. Palacin, and B. Jousselme, "Relationship between polypyrrole morphology and electrochemical activity towards oxygen reduction reaction.," *Chem. Commun.*, vol. 48, no. 38, pp. 4627–4629, 2012.
- [3] E. Raymundo-Piñero, D. Cazorla-Amorós, Á. Linares-Solano, J. Find, U. Wild, and R. Schlogl, "Structural characterization of N-containing activated carbon fibers prepared from a low softening point petroleum pitch and a melamine resin," *Carbon*, vol. 40, pp. 597–608, 2002.
- [4] E. Raymundo-Piñero, D. Cazorla-Amorós, and Á. Linares-Solano, "The role of different nitrogen functional groups on the removal of SO<sub>2</sub> from flue gases by N-doped activated carbon powders and fibres," *Carbon*, vol. 41, no. 10, pp. 1925–1932, 2003.
- [5] P. Trogadas, T. F. Fuller, and P. Strasser, "Carbon as catalyst and support for electrochemical energy conversion," *Carbon*, vol. 75, pp. 5–42, 2014.
- [6] P. Zhang, F. Sun, Z. Xiang, Z. Shen, J. Yun, and D. Cao, "ZIF-derived in situ nitrogen-doped porous carbons as efficient metal-free electrocatalysts for oxygen reduction reaction," *Energy Environ. Sci.*, vol. 7, no. 1, pp. 442–450, 2014.

Full Thesis can be downloaded from:

<https://rua.ua.es/dspace> or [www.ua.es](http://www.ua.es)

## **Socios protectores del Grupo Español del carbón**